Charged Higgs Phenomenology of the Lepton-Specific and Flipped Two Higgs Doublet Models

by

Deanna MacLennan

A thesis submitted to the
Faculty of Graduate Studies and Research
in partial fulfillment of the requirements
for the degree of
Master of Science

Department of Physics
Carleton University
Ottawa-Carleton Institute of Physics
Ottawa, Canada

August 24, 2009

Your file Votre référence
ISBN: 978-0-494-60134-1
Our file Notre référence
ISBN: 978-0-494-60134-1

Abstract

The lepton-specific and flipped two Higgs doublet models (2HDMs) are studied. The lepton-specific two Higgs doublet model (2HDM-L) is a 2HDM in which one doublet Φ_ℓ couples to leptons and the other doublet Φ_q couples to both up- and down-type quarks; in the flipped 2HDM (2HDM-F) Φ_d couples to down-type quarks while $\Phi_{u,\ell}$ couples to up-type quarks and leptons. For both models, existing experimental constraints are used to constrain the charged Higgs mass and the parameter $\tan\beta$. The LEP-II direct search gives a lower bound $M_{H^\pm} \geq 92.0$ (78.0) GeV for the lepton-specific (flipped) 2HDM. The strongest indirect constraint in the flipped model comes from $b \to s\gamma$ which gives $M_{H^\pm} \geq 295$ GeV; the most stringent constraint in the lepton-specific model comes from lepton universality in tau decays which gives $0.61 \tan\beta$ GeV $\leq M_{H^\pm} \leq 0.73 \tan\beta$ GeV or $M_{H^\pm} \geq 1.4 \tan\beta$ GeV at the 95% confidence level. Charged Higgs decay branching fractions are presented for both models and the potential discovery processes at the LHC are examined.

Acknowledgements

I would like to thank my supervisor, Dr. Heather Logan, whose expertise, understanding, and guidance, have made my graduate degree a great experience. I admire her vast knowledge in all areas of physics, her positive attitude, and her ability to explain complicated theories. She is an exceptional person, as well as teacher, and it has been an honour to work with her.

Statement of Originality

The results in this thesis are either entirely the work of the author, or a summary of work by others appropriately referenced where applicable.

Much of the work in Chapter 2 has been published in the reference listed below. Although the paper was co-authored with Heather Logan, the work appearing in this thesis is entirely my own and any work I did not contribute to is referenced as such.

Previously Published Paper

H. E. Logan and D. MacLennan, Phys. Rev. D **79**, 115022 (2009) [arXiv:0903.2246 [hep-ph]].

Contents

List of Tables

List of Figures

Chapter 1

Introduction

The Standard Model (SM) is the theory upon which all of particle physics is based. The SM uses the mathematical framework of quantum field theory and applies it to the forces of nature that are fundamental to physics. All interactions experienced by humans in day to day life are the product of elementary particles obeying the four fundamental forces: the strong, weak, electromagnetic, and gravitational forces. Each of these forces has its own function within the complexities of nature, and has its own unique role in the interactions of particles. The strong and weak forces describe the interaction of particles at the most microscopic level while the electromagnetic force describes the interaction of atoms; the gravitational force determines the rules of attraction for large bodies. The strong force, for instance, binds the nucleons within the nucleus so tightly that the electromagnetic repulsion of protons does not rip apart the atom. The weak force governs leptonic decays such as beta decay and gravity keeps the earth in orbit around the sun.

1.1 The Framework

Quantum field theory is the mathematical structure which the SM is based upon. Contrary to classical mechanics, quantum mechanics proposes that when finding the probability between two events every path must be kept such that

$$P = \left[\sum_{all\ paths} e^{-iS} \right]^2 \tag{1.1}$$

where the path is defined to be the exponential of the action S.

In quantum field theory Eq. 1.1 is replaced by the functional integral. A functional integral is an infinite set of integrals which account for every possible field configuration at every single point in 4-dimensional space. Every field configuration will contribute to the integral to a degree depending on the value of the action corresponding to that specific field configuration. As an example, consider a theory containing a spin zero quantum field ϕ and a spin one field A_μ; for this theory the functional integral would be represented as

$$P = \int [D\phi][DA_\mu] e^{-iS}. \tag{1.2}$$

Equation 1.2 is an infinite expansion of e^{-iS} which can not be solved exactly. A mathematical tool used for calculating this expansion is to organize the terms in a series of Feynman diagrams. The diagrams themselves are an infinite expansion where the order is denoted by the number of loops involved. The lowest order diagram allowed by conservation laws is the tree-level diagram of a propagator exchanged between two particles. From here, the next order has one loop, followed by two loops, etc. For every loop order there is an increasing number of potential diagrams, and

the calculated precision of the quantum effect is determined by the number of loops that one calculates.

The Feynman rules for the diagram are found from the Lagrangian density of the theory. The action is related to the Lagrangian density $\mathcal{L}$ through the equation

$$S = \int d^4x \quad \mathcal{L}. \tag{1.3}$$

The Lagrangian can be written in sections of increasing order in the fields. To find the rule for the propagator we take terms from the Lagrangian bilinear in the fields and write them in the form where there is an operator acting upon the two fields. This operator is then inverted to obtain the propagator.

The terms in the Lagrangian that have more powers of the field give rise to interactions. These interactions correspond to the vertices of Feynman diagrams, so in order to obtain the vertex rules for the diagrams we must proceed with these terms in the same fashion described for the propagator.

In order to find a quantum theory for each of the classical forces, one begins with the Lagrangian associated with that force and derives the Feynman rules. The Lagrangian will always involve derivatives and terms involving the masses and couplings of the theory. As an example, consider ϕ^4 theory. The Lagrangian for ϕ^4 theory is

$$\mathcal{L} = \frac{1}{2}(\partial_\mu \phi)^2 - \frac{1}{2}m^2\phi^2 - \frac{\lambda}{4!}\phi^4 \tag{1.4}$$

where λ is a dimensionless constant and m is a constant with dimensions of mass. In Eq. 1.4 the first term contains the derivative of the scalar field, the second is the mass term and the last term gives the interaction behaviour of the theory. Written

in this form one can read the mass as m from the term bilinear in the field, and the Feynman rule for the coupling of 4 fields is $-i\lambda$. These masses and couplings are really just arbitrary constants which must be fixed by experiment. In order to match these constants to experimental results, one must calculate a scattering amplitude which typically involves divergent loop integrals. In order to avoid this problem, physicists introduce a cutoff to their divergent integral which allows them to find cutoff dependent values for the desired constants which can be used again for calculations of the same order. If, in the subsequent calculations, it is possible to get a cutoff independent scattering amplitude then one is dealing with what is called a renormalizable field theory. This is in fact the necessary condition to be a quantum field theory in the Standard Model; the theory must be renormalizable. On imposing this restriction a major flaw was discovered - only three of the four fundamental forces become a renormalizable field theory and gravity is not part of the SM. This was the first sign that the Standard Model could not be the full description of nature, but a subset of a more complex creature.

1.1.1 Gauge Theory

A gauge field is a field which can have different configurations that all have the same action. The way in which one can arrive at a new field configuration without affecting the action is called a gauge transformation. By integrating over all of these values within the gauge field it is possible to get multiple copies of the same form, which is not the desired calculation. One should only integrate over those values of the gauge field which give unique results. By fixing the gauge one can accomplish just that.

1.1.11. Gauge Invariance of the Dirac Field

The Dirac Lagrangian is given as

$$\mathcal{L} = i\bar{\psi}\gamma^{\mu}\partial_{\mu}\psi - m\bar{\psi}\psi. \tag{1.5}$$

In order to describe the interactions of the Dirac field with a gauge field, we will require the Lagrangian to be invariant under the local gauge transformation $\psi \rightarrow e^{i\omega(x)}$. Under such a transformation the Lagrangian is modified as

$$\mathcal{L} \rightarrow \mathcal{L} + (\bar{\psi}\gamma^{\mu}\psi)\partial_{\mu}\omega(x) \tag{1.6}$$

and in order for it to be invariant a counter term must be added to the original Lagrangian. Modifying Eq.1.5 by adding a term including a 'gauge' field, A_{μ} which transforms according to $A_{\mu} \rightarrow A_{\mu} + \partial_{\mu}\omega(x)$, the new Lagrangian is written as

$$\mathcal{L}' = i\bar{\psi}\gamma^{\mu}\partial_{\mu}\psi - m\bar{\psi}\psi - \bar{\psi}\gamma^{\mu}\psi A_{\mu}. \tag{1.7}$$

If we replace the normal derivative with the covariant derivative $\partial_{\mu} \rightarrow \mathcal{D}_{\mu} = \partial_{\mu} + iA_{\mu}$ then the new Lagrangian is written as

$$\mathcal{L} = i\bar{\psi}\gamma^{\mu}\mathcal{D}_{\mu}\psi - m\bar{\psi}\psi \tag{1.8}$$

and is invariant under a local transformation $\psi \rightarrow e^{i\omega(x)}$ as desired. This is an example of a $U(1)$ gauge theory because the gauge transformation is described by one complex function $e^{i\omega(x)}$, which for a given $\omega(x)$ choice is equivalent to a 1×1 unitary matrix.

Other gauge theories can be constructed using more complicated group structure for the gauge transformations. Consider an $SU(N)$ theory with $e^{igT^a\omega^a(x)}$ in which T^a are the generators of the $SU(N)$ group algebra. In this theory, ψ is now a multi-element object that transforms under some representation of the SU(N) gauge group. As an example consider the $SU(3)_C$ structure of quantum chromodynamics (QCD). The field ψ is now written as

$$\psi_i = \begin{pmatrix} q_i^R \\ q_i^B \\ q_i^G \end{pmatrix} \tag{1.9}$$

where the index, i, denotes the quark flavor, and R, B, G stand for red, blue, and green color respectively. The global $SU(3)_C$ transformation is given by

$$\psi_i \rightarrow \psi_i' = \exp(-i\theta \cdot \lambda/2)\ \psi_i \tag{1.10}$$

where θ_α (α= 1, 2,..., 8) is the general $SU(3)_C$ matrix and the λ^α are 3×3 Gell-Mann matrices which generalise the τ^α Pauli matrices of $SU(2)$. Imposing the invariance of Eq. 1.10 holds locally ($\theta \rightarrow \theta(x)$), the invariant $SU(3)_C$ Lagrangian is written as

$$\mathcal{L} = \bar{\psi}_i(i\not{\partial} - m_i - g_s\frac{\lambda^\alpha}{2}\not{A}^\alpha)\psi_i - \frac{1}{4}F^\alpha_{\mu\nu}F^{\alpha\mu\nu} \tag{1.11}$$

where g_s is the strong gauge coupling and $F^\alpha_{\mu\nu} = \partial_\mu A^\alpha_\nu - \partial_\nu A^\alpha_\mu - g_s f_{\alpha\beta\gamma} A^\beta_\mu A^\gamma_\nu$ is the strong interaction field strength tensor. The covariant derivative is now defined as $\mathcal{D}_\mu = \partial_\mu + ig_s\frac{\lambda^\alpha}{2}A^{\alpha\mu}$ and there are 8 gauge fields $A^{\alpha\mu}$ that correspond to the 8 gluons which mediate the strong interaction.

1.2 Electroweak Symmetry Breaking

The second major stumbling block for the SM came with the unification of the electromagnetic and weak interactions. If there were to be an exact electroweak symmetry then the photon, $W^{\pm}$ boson, and Z boson would all have to be massless. The mass of the $W^{\pm}$ boson and the Z boson are known from experiment to be 80 GeV and 91 GeV respectively [1] which contradicts this unification. The idea proposed was that at low energies the $SU(2)_L \times U(1)_Y$ (L denoting the weak interactions favoring left handed fermions, and Y denoting hypercharge) symmetry must be broken down to the $U(1)_{EM}$ symmetry observed in nature [2].

1.2.1 The Higgs Mechanism

Consider a set of scalars which transform under a symmetry. When the symmetry is spontaneously broken, the scalars get a vacuum expectation value (vev) in a given direction. Goldstone's theorem [3] states that when the symmetry is broken, the scalars which correspond to the other directions come out as massless scalar particles called Goldstone bosons. If the symmetry is gauged the would-be scalars are 'eaten' by the gauge bosons as the third polarization state required by a massive spin 1 particle; this is the Higgs mechanism [4]. In other words particles aquire mass by interacting with the background Higgs field which has a non-zero vev.

As an example, I will show how to use the Higgs mechanism to break a $U(1)$ gauge symmetry. The kinetic Lagrangian of a $U(1)$ gauge theory is

$$\mathcal{L} = -\frac{1}{4} F^{\mu\nu} F_{\mu\nu}, \tag{1.12}$$

where $F^{\mu\nu} = \partial^{\mu} A^{\nu} - \partial^{\nu} A^{\mu}$. A mass term $\frac{1}{2} m^2 A^{\mu} A_{\mu}$ is not allowed in a U(1) gauge

theory since the Lagrangian must be invariant under the transformation $A^\mu(x) \rightarrow A^\mu(x) - \partial^\mu\omega(x)$ for any field $\omega(x)$. According to gauge invariance the photon must remain massless, however it is possible to add a complex scalar field ϕ modifying the Lagrangian to be [5]

$$\mathcal{L} = -\frac{1}{4}F^{\mu\nu}F_{\mu\nu} + |\mathcal{D}_\mu\phi|^2 - V(|\phi|^2). \tag{1.13}$$

In this unrealistic example, the covariant derivative is defined to be $\mathcal{D}_\mu = \partial_\mu - ieA_\mu$, and the most general scalar potential is

$$V(|\phi|^2) = \mu^2|\phi|^2 + \lambda(|\phi|^2)^2. \tag{1.14}$$

The U(1) symmetry is spontaneously broken when μ^2 is negative. By minimizing the potential the vev is found to be $\langle\phi\rangle \equiv v = \sqrt{-\frac{\mu^2}{2\lambda}}$. Now it is possible to define a field $\varphi = \phi - v$, which upon substituting into Eqn. 1.13 gives bilinear terms in the Lagrangian [5]

$$\begin{aligned}\mathcal{L}_\varphi &= -\frac{1}{4}F^{\mu\nu}F_{\mu\nu} + \partial_\mu\varphi^*\partial^\mu\varphi + ieA_\mu(v\partial^\mu\varphi^* - v^*\partial^\mu\varphi) - e^2v^*vA_\mu A^\mu \\ &\quad -\lambda(v^*\varphi + v\varphi^*)^2.\end{aligned} \tag{1.15}$$

Finally, in order to read off the particle masses, U(1) gauge transformations $A_\mu(x) \rightarrow A_\mu(x) + \partial_\mu\omega(x)$ and $\phi(x) \rightarrow e^{ie\omega(x)}\phi(x)$ are used to constrain $\phi = \phi^*$. This gauge choice is called the Unitary gauge and eliminates the 3rd term in the ground state Lagrangian which includes scalar and vector fields. Imposing this condition, the ground state Lagrangian now reads

$$\mathcal{L}_\varphi = -\frac{1}{4}F^{\mu\nu}F_{\mu\nu} + \partial_\mu\varphi\partial^\mu\varphi - e^2v^2A_\mu A^\mu - 4v^2\lambda\varphi^2 \tag{1.16}$$

and the particle masses can be read off as $M_{A_\mu}^2 = 2e^2v^2$, $M_\varphi^2 = 4\lambda v^2$.

The above example, while unrealistic, shows the Higgs mechanism at work in a simple U(1) gauge theory. In the following section this same procedure will be used to give mass to the $W^\pm$ and Z bosons by breaking a $SU(2)_L \times U(1)_Y$ gauge theory.

1.3 Salam - Weinberg Theory

The accepted Standard Model electroweak theory is called the Salam-Weinberg theory [6], after two physicists who first applied the Higgs mechanism to a $SU(2)_L \times U(1)_Y$ gauge theory. From group theory we know that every group of the form $SU(N)$ has $N^2 - 1$ generators which correspond to the number of force mediators of that group. Electroweak theory has 3 $SU(2)_L$ generators and 1 $U(1)_Y$ generator corresponding to the gauge bosons W_μ^a $(a = 1, 2, 3)$, and B_μ hypercharge respectively. The most general gauge invariant Lagrangian for this theory is [5]

$$\mathcal{L}_{SW} = -\frac{1}{4} W_{\mu\nu}^a W^{a\mu\nu} - \frac{1}{4} B_{\mu\nu} B^{\mu\nu} \tag{1.17}$$

where $W_{\mu\nu}^a$ and $B_{\mu\nu}$ are defined as

$$W_{\mu\nu}^a = \partial_\mu W_\nu^a - \partial_\nu W_\mu^a + g\epsilon_{abc} W_\mu^b W_\nu^c \,, \qquad B_{\mu\nu} = \partial_\mu B_\nu - \partial_\nu B_\mu, \tag{1.18}$$

g is the $SU(2)_L$ gauge coupling and ϵ_{abc} is a totally antisymmetric tensor. Analogous to the Higgs mechanism described for giving mass to the photon, in order to break the electroweak symmetry a complex scalar field is introduced. For a $SU(2)_L \times U(1)_Y$ theory it is necessary to introduce a doublet of hypercharge Y=1. From the relation $Q = T_3 + Y/2$, where Q is the electric charge and T_3 is the third component of isospin,

the doublet must be written as

$$\phi = \begin{pmatrix} \phi^+ \\ \phi^0 \end{pmatrix}. \tag{1.19}$$

Including this new scalar field the Lagrangian now reads

$$\mathcal{L} = \mathcal{L}_{Higgs} + \mathcal{L}_{SW} = (D_\mu \phi)^\dagger (\mathcal{D}^\mu \phi) - V(\phi^\dagger \phi) - \frac{1}{4} W^a_{\mu\nu} W^{a\mu\nu} - \frac{1}{4} B_{\mu\nu} B^{\mu\nu} \tag{1.20}$$

where the SM covariant derivative for ϕ is given by

$$\mathcal{D}_\mu = \partial_\mu - \frac{i}{2} g W^a_\mu \tau_a - \frac{i}{2} g' B_\mu \tag{1.21}$$

where τ_a are the Pauli matrices, g [g'] are the SU(2) [U(1)] weak couplings, and the scalar potential is given by Eq. 1.30. To find the masses of the observable bosons, one can write the Higgs doublet in the Unitary gauge

$$\phi = \begin{pmatrix} 0 \\ \frac{1}{\sqrt{2}}(v+h) \end{pmatrix}, \tag{1.22}$$

and expand the terms in the covariant derivative and scalar potential of $\mathcal{L}_{higgs}$ to get

$$\begin{aligned} (D_\mu \phi)^\dagger (\mathcal{D}^\mu \phi) - V(\phi^\dagger \phi) \;=\; & -\frac{1}{2} \partial_\mu h \partial^\mu h - \lambda v^2 h^2 - \lambda v h^3 - \frac{\lambda}{4} h^4 \\ & -\frac{1}{8} g^2 (v+h)^2 |W^1_\mu - i W^2_\mu|^2 \\ & -\frac{1}{8} (v+h)^2 (g W^3_\mu - g' B_\mu)^2. \end{aligned} \tag{1.23}$$

The physical bosons observed in nature are not the generators $W^a_{\mu\nu}$ and B_μ from the above expression, but rather the linear combinations of these generators appearing in

Eq. 1.23 defined as [7]

$$W_\mu^\pm = \frac{1}{\sqrt{2}}(W_\mu^1 \mp iW_\mu^2), \qquad Z_\mu = \frac{gW_\mu^3 - g'B_\mu}{\sqrt{g^2+g'^2}}, \qquad A_\mu = \frac{g'W_\mu^3 + gB_\mu}{\sqrt{g^2+g'^2}}.$$

Substituting these expressions into Eq. 1.23 the masses of the observable bosons are read off to be

$$M_{W^\pm}^2 = \frac{g^2v^2}{4}, \qquad M_Z^2 = \frac{1}{4}(g^2+g'^2)v^2, \qquad M_A^2 = 0. \tag{1.24}$$

As expected, the photon A_μ is massless since the symmetry of electromagnetism is not broken by the choice of vacuum expectation value. Since the masses of the $W^\pm$ and Z bosons as well as the weak coupling constants g, and g', are experimentally known, this approximately determines the value of the SM vev to be 246 GeV.

1.4 Two Higgs Doublet Models

In the Standard Model there is no restriction on only having a single complex scalar doublet that spontaneously breaks the electroweak symmetry. There is however a restriction placed on how you can extend this minimal choice. In the SM there is a parameter, ρ defined as

$$\rho = \frac{M_W^2}{M_Z^2 \cos^2\theta_W} \tag{1.25}$$

which is experimentally known to be close to 1. Since the masses of the W and Z bosons and Weinberg angle, θ_W, can not change between models, the ρ parameter must also equal 1 in extended Higgs models. In extended Higgs models containing only Higgs doublets, the value of ρ is automatically 1, so two Higgs doublet models are theoretically allowed and will be studied in this thesis.

In any 2HDM, the two complex Higgs $SU(2)$-doublets are once again constrained by the relation $Q = T_3 + Y/2$ and are written in the gauge basis as

$$\Phi_\alpha = \begin{pmatrix} \phi_\alpha^+ \\ \frac{1}{\sqrt{2}}\left(\phi_\alpha^{0,r} + v_\alpha + i\phi_\alpha^{0,i}\right) \end{pmatrix}, \tag{1.26}$$

where $\alpha = 1, 2$ denotes the specific doublet. The neutral component of the doublet has been broken down into real and imaginary components because the observable particles in the mass basis are linear combinations of these fields, so by writing them in this form it is easier to identify and work with a given observable.

A two Higgs doublet model has 8 scalar degrees of freedom which combine to give 5 physical Higgs particles, and 3 unphysical fields (the Goldstone bosons). The observable particles can be written in terms of the original fields as

$$\begin{aligned} A^0 &= -\phi_1^{0,i}\sin\beta + \phi_2^{0,i}\cos\beta, \\ H^0 &= \phi_1^{0,r}\cos\alpha + \phi_2^{0,r}\sin\alpha, \\ h^0 &= -\phi_1^{0,r}\sin\alpha + \phi_2^{0,r}\cos\alpha, \\ H^+ &= -\phi_1^{+}\sin\beta + \phi_2^{+}\cos\beta, \\ H^- &= -\phi_1^{-}\sin\beta + \phi_2^{-}\cos\beta. \end{aligned} \tag{1.27}$$

Here β is the mixing angle that diagonalizes the mass matrices for the CP-odd and charged states, while α rotates between the gauge and mass basis of the CP-even states. The neutral Goldstone boson, G^0, is defined to be orthogonal to A^0 and the charged Goldstone boson, $G^\pm$, is defined to be orthogonal to $H^\pm$. In order to find the Feynman rules for a given observable, it is possible to neglect certain fields in Eqn. 1.26 and work only with those fields which comprise the particle in question.

The full Lagrangian for the two Higgs doublet model (2HDM) is

$$\mathcal{L}_{2HDM} = \mathcal{L}_{EW} + \mathcal{L}_{Higgs}. \tag{1.28}$$

The electroweak piece of the Lagrangian is the same as in the Salam-Weinberg theory and the Higgs piece of the Lagrangian has been modified to include two Higgs doublets. In the study of 2HDM's $\mathcal{L}_{EW}$ gives no new information on the Higgs sector of the theory, so it is simpler to focus only on $\mathcal{L}_{Higgs}$. Including both doublets the form of the Higgs Lagrangian is [8,9]

$$\mathcal{L}_{Higgs} = \mathcal{L}_{Kinetic} - V_{Scalar} + \mathcal{L}_{Yukawa} \tag{1.29}$$

where $\mathcal{L}_{Kinetic} = |\mathcal{D}_\mu \Phi_1|^2 + |\mathcal{D}_\mu \Phi_2|^2$. The most general form of the scalar potential is given in Ref. [10]. Imposing CP-conservation and a $\mathbb{Z}_2$ symmetry we obtain,

$$\begin{aligned} V_{Scalar} &= m_{11}^2 \Phi_1^\dagger \Phi_1 + m_{22}^2 \Phi_2^\dagger \Phi_2 - \left(m_{12}^2 \Phi_1^\dagger \Phi_2 + h.c. \right) + \frac{\lambda_1}{2} \left(\Phi_1^\dagger \Phi_1 \right)^2 \\ &+ \frac{\lambda_2}{2} \left(\Phi_2^\dagger \Phi_2 \right)^2 + \lambda_3 \left(\Phi_1^\dagger \Phi_1 \right) \left(\Phi_2^\dagger \Phi_2 \right) + \lambda_4 \left(\Phi_2^\dagger \Phi_1 \right) \left(\Phi_1^\dagger \Phi_2 \right) \\ &+ \left[\frac{\lambda_5}{2} \left(\Phi_1^\dagger \Phi_2 \right)^2 + h.c. \right], \end{aligned} \tag{1.30}$$

where *h.c.* denotes the Hermitian conjugate.

In Eq. 1.30 the $\mathbb{Z}_2$ symmetry is softly-broken by the third term $\left(m_{12}^2 \Phi_1^\dagger \Phi_2 + h.c. \right)$. The constraint that only dimension-two terms are allowed to violate the $\mathbb{Z}_2$ symmetry keeps flavor-changing neutral currents (FCNCs) small which is required since FCNCs are suppressed in the SM.

As long as each doublet aquires a vev then they will both contribute to the masses

of the gauge bosons. Similar to the Salam-Weinberg theory, the masses of the gauge bosons are determined from the kinetic piece of the Lagrangian. In a 2HDM, the kinetic Lagrangian has two terms involving the covariant derivative. In order to derive the mass of the bosons, any terms of Eqn. 1.26 which include a field can be set to zero since mass terms are bilinear in the field of the particle in question. Setting all terms except the vev to zero Φ_α can be written as

$$\Phi_\alpha = \begin{pmatrix} 0 \\ \frac{v_\alpha}{\sqrt{2}} \end{pmatrix}. \tag{1.31}$$

Applying the SM covariant derivative on Eqn. 1.31 gives

$$\mathcal{D}_\mu \Phi_\alpha = -\frac{i}{2\sqrt{2}} \begin{pmatrix} gW_\mu^3 + g'B_\mu & gW_\mu^1 - igW_\mu^2 \\ gW_\mu^1 + igW_\mu^2 & -gW_\mu^3 + g'B_\mu \end{pmatrix} \begin{pmatrix} 0 \\ v_\alpha \end{pmatrix},$$

and consequently

$$|\mathcal{D}_\mu \Phi_\alpha|^2 = \frac{v_\alpha^2}{8} \left[(gW_\mu^1 - igW_\mu^2)(gW^{1\mu} + igW^{2\mu}) + (-gW_\mu^3 + g'B_\mu)(-gW^{3\mu} + g'B^\mu) \right]. \tag{1.32}$$

Substituting Eqn. 1.32 into the kinetic piece of the Higgs Lagrangian,

$$|\mathcal{D}_\mu \Phi_1|^2 + |\mathcal{D}_\mu \Phi_2|^2 = \frac{1}{8} g^2 (v_1^2 + v_2^2) |W_\mu^1 - iW_\mu^2|^2 + \frac{1}{8} (v_1^2 + v_2^2)(-gW_\mu^3 + g'B_\mu)^2 \tag{1.33}$$

where once again the mass terms can be read off as

$$M_Z^2 = \frac{1}{4}(g^2 + g'^2)(v_1^2 + v_2^2), \qquad M_{W^\pm}^2 = \frac{1}{4} g^2 (v_1^2 + v_2^2). \tag{1.34}$$

Comparing the masses of the $W^\pm$ and Z bosons derived from a model with two Higgs doublets to the Salam-Weinberg theory, the value of the two vevs are constrained by

	2HDM-I	2HDM-II	2HDM-L	2HDM-F
Φ_1	-	d, ℓ	ℓ	d
Φ_2	u, d, ℓ	u	u, d	u, ℓ

Table 1.1: Possible 2HDMs which avoid flavor changing neutral currents (FCNCs).

the Standard Model vev through the relation

$$v_1^2 + v_2^2 = v^2. \tag{1.35}$$

Conventionally, Eq. 1.35 is used to define the ratio of the vevs [8, 11]

$$\frac{v_2}{v_1} = \tan\beta \tag{1.36}$$

and $\tan\beta$ is then used as a parameter of the theory. Due to the structure of the theory this angle β is the same as the mixing angle for the A^0, G^0 and $H^\pm$, $G^\pm$ Higgs particles given in Eq. 1.27.

Until this point the Yukawa Lagrangian has not been defined. This is because the Yukawa Lagrangian is model dependent and it is a choice which doublet couples to which type of fermions. There are 4 possible Yukawa structures which obey the Glashow-Weinberg-Paschos condition for natural flavour conservation [12, 13]. This condition requires that each fermion type receive mass from exactly one Higgs doublet. The four possible models are summarized in Table 1.1 with u, d, ℓ, representing the up-type fermions, down-type fermions and leptons respectively. There is also the Type-III 2HDM which does not obey the Glashow-Weinberg-Paschos condition for natural flavour conservation, however this model is beyond the scope of this thesis.

While the 2HDM-I and 2HDM-II have been widely studied and documented, there are two other models which have interesting phenomenology and have yet to be studied

in detail. There is a leptonic' or lepton-specific two Higgs doublet model (2HDM-L) in which one doublet couples to leptons while the other couples to quarks, and a flipped 2HDM (2HDM-F) in which one doublet couples to down-type quarks and the other couples to up-type quarks and leptons. The main focus of this thesis will be to study charged Higgs phenomenology in these two models and how the constraints compare to those already published in the literature. Here we briefly review the Yukawa structure of the Type-I and Type-II models.

1.4.1 Type-I 2HDM

The Type-I 2HDM (2HDM-I) has been extensively studied in the literature (see Ref. [8, 14]), and constraints from low energy processes have been known for the last 20 years. The 2HDM-I has one doublet Φ_2 which couples to fermions while the other doublet Φ_1 decouples completely from the fermion sector. The Yukawa Lagrangian for this model is

$$\mathcal{L}_{2HDM-I} = -\sum_{i=1}^{3}\sum_{j=1}^{3}\left[y_{ij}^{u}\overline{Q}_{Li}\tilde{\Phi}_2 u_{Rj} + y_{ij}^{d}\overline{Q}_{Li}\Phi_2 d_{Rj} + y_{ij}^{\ell}\overline{L}_{Li}\Phi_2 \ell_{Rj}\right] + h.c. \qquad (1.37)$$

where $i,\ j$ are generation indices, y_{ij}^{α} are Yukawa couplings, the conjugate doublet $\tilde{\Phi}$ is defined as

$$\widetilde{\Phi}_\alpha = i\sigma_2\Phi_\alpha^* = \begin{pmatrix} \frac{1}{\sqrt{2}}\left(\phi_\alpha^{0,r} + v_\alpha - i\phi_\alpha^{0,i}\right) \\ -\phi_\alpha^- \end{pmatrix}, \qquad (1.38)$$

the left-handed lepton and quark doublets are denoted by

$$L_L = \begin{pmatrix} \nu_L \\ \ell_L \end{pmatrix}, \quad Q_L = \begin{pmatrix} u_L \\ d_L \end{pmatrix},$$

and $u_R,\ d_R$, and ℓ_R denote the right-handed $SU(2)_L$ – singlet fermions.

The $H^{\pm}$ part of the Yukawa Lagrangian is

$$\mathcal{L}_{2HDM-I} = \frac{g}{\sqrt{2}M_W} H^{+} \left[V_{ij} m_{ui} \cot\beta \bar{u}_i P_L d_j - V_{ij} m_{dj} \cot\beta \bar{u}_i P_R d_j - m_{li} \cot\beta \bar{\nu}_i P_R \ell_i \right] + h.c, \tag{1.39}$$

and the relevant couplings are [15]

$$\begin{aligned} H^{+}\bar{u}_i d_j &= \frac{ig}{\sqrt{2}M_W} V_{ij} \cot\beta (m_{ui} P_L - m_{dj} P_R) \\ H^{+}\bar{\nu}_i \ell_i &= -\frac{ig}{\sqrt{2}M_W} \cot\beta m_{\ell i} P_R. \end{aligned} \tag{1.40}$$

Here V_{ij} is the appropriate Cabibbo-Kobayashi-Maskawa (CKM) matrix element (see Sec. 2.1.31.) and $P_{L,R} = (1 \mp \gamma_5)/2$ are the left- and right-handed projection operators. m_{ui}, m_{di} are the mass of the up-type and down-type quarks respectively, $m_{\ell i}$ is the mass of the leptons and in all cases i denotes the specific generation.

1.4.2 Type-II 2HDM

The Type-II 2HDM (2HDM-II) is the most widely studied and accepted model since it is compatible with the minimal supersymmetric Standard Model (see Ref. [9, 11, 16, 17]). The 2HDM-II has one doublet Φ_2 which couples to up-type quarks while the second doublet Φ_1 couples to down-type quarks and leptons. The Yukawa Lagrangian for this model is

$$\mathcal{L}_{2HDM-II} = -\sum_{i=1}^{3}\sum_{j=1}^{3} \left[y^{u}_{ij} \overline{Q}_{Li} \tilde{\Phi}_2 u_{Rj} + y^{d}_{ij} \overline{Q}_{Li} \Phi_1 d_{Rj} + y^{\ell}_{ij} \overline{L}_{Li} \Phi_1 \ell_{Rj} \right] + h.c. \tag{1.41}$$

where the $H^{\pm}$ part is

$$\mathcal{L}_{2HDM-II} = \frac{g}{\sqrt{2}M_W} H^+ \left[V_{ij} m_{ui} \cot\beta \bar{u}_i P_L d_j + V_{ij} m_{dj} \tan\beta \bar{u}_i P_R d_j + m_{\ell i} \tan\beta \bar{\nu}_i P_R \ell_i\right] + h.c. \tag{1.42}$$

and the relevant couplings are [15]

$$\begin{aligned} H^+ \bar{u}_i d_j &= \frac{ig}{\sqrt{2}M_W} V_{ij} (\cot\beta m_{ui} P_L + \tan\beta m_{dj} P_R) \\ H^+ \bar{\nu}_i \ell_i &= \frac{ig}{\sqrt{2}M_W} \tan\beta m_{\ell i} P_R. \end{aligned} \tag{1.43}$$

The derivation of the Yukawa Lagrangian and Higgs couplings will be further discussed in Sec. 2.1.31.

1.4.3 The Outline

In Chapter 2 we study the Leptonic, or Lepton-Specific, 2HDM.

- In Sec. 2.1 the main framework of the 2HDM-L is reviewed. The perturbativity of the τ Yukawa coupling is used to constrain the range of the free parameter $\tan\beta$. An example of diagonalising mass matrices is given and then applied to the lepton-specific model. The Feynman rules for the charged Higgs couplings are then explored with an emphasis on the CKM matrix.

- Section 2.2 summarizes the existing constraints from the literature as well as new model specific constraints. A lower bound of $M_{H^\pm} \geq 92.0$ GeV is found from the LEP Collaborations and the strongest indirect constraint from lepton universality in tau decays is calculated. Constraints from Michel parameters are shown to be weaker than the LEP bound and constraints from other low

energy processes are studied and found to be uninteresting. Finally, constraints from the Tevatron experiment are analyzed and found to be irrelevant since the area of parameter space constrained is already disfavoured by $b \to s\gamma$.

- Section 2.3 displays plots of the charged Higgs branching ratios and total width as a function of $M_{H^\pm}$for $\tan\beta = 5$, 10, 20, and 100. The model specific signatures are examined and compared to those of the Type-II 2HDM.

- In Sec. 2.4 we study LHC search prospects. The current studies by the ATLAS and CMS experiments, and how they apply to the lepton-specific model, are summarized. The light and heavy charged Higgs mass ranges are examined, and a plot of cross sections for relevant processes is shown. Because $H^\pm$ couplings to quarks tend to be suppressed in this model, the most important production modes involve electroweak couplings; e.g., $pp \to H^+H^- \to \tau\nu\tau\nu$.

In Chapter 3 we study the Flipped 2HDM.

- Section 3.1 reviews the main framework of the Flipped 2HDM. The perturbativity of the top and bottom Yukawa couplings are then used to constrain the range of the free parameter $\tan\beta$.

- Section 3.2 summarizes the existing constraints from the literature as well as new model specific constraints. A $BR(H^+ \to \tau^+\nu)$ independent lower bound of $M_{H^\pm} \geq 78.0$ GeV is found from the LEP Collaborations. The strongest indirect constraint from $b \to s\gamma$ is given in detail. Constraints from other low energy processes are studied and found to be insignificant. Finally, upper and lower bounds on $\tan\beta$ are found from the upper limit on the branching ratio $BR(t \to H^\pm b)$ from the Tevatron.

- Section 3.3 displays plots of the charged Higgs branching ratios and total width as a function of $M_{H^\pm}$ for $\tan\beta = 1$, 5, 10, and 50. The model specific signatures are examined and compared to those of the Type-II 2HDM.

- Section 3.4 summarizes the current studies by ATLAS and CMS and how they can be applied to the Flipped model. The light and heavy charged Higgs mass ranges are examined, and a plot of cross sections for relevant processes is shown. The dominant process is found to be bottom-gluon fusion $gb \rightarrow tH^+$ as is the case in the Type-II model.

Chapter 4 gives a short summary of the results and discusses the differences between the Lepton-Specific, Flipped and the Type-II models.

Chapter 2

The Lepton-Specific 2HDM

In the lepton-specific 2HDM (2HDM-L), one doublet gives mass to up- and down-type quarks while the other gives mass to leptons. This model was first proposed in Refs. [18,19,20] ; studies of detecting this model at the Large Electron Positron (LEP) collider were made in Ref. [21], and more detailed studies of branching ratios, LEP constraints, and LHC search prospects were made in Refs. [22,23,24,25,26,27,28]. In this chapter we outline the main features of the 2HDM-L in the charged Higgs sector; we give constraints adapted from the LEP-II direct search, as well as constraints from lepton universality in muon and tau decays, Michel parameters, and other low energy processes. Finally we investigate charged Higgs decay branching ratios as a function of $M_{H^\pm}$ for $\tan\beta = 5,\ 10,\ 20,$ and 100 and discuss the production processes at the Large Hadron Collider (LHC). The results from lepton universality, Michel parameters, $B^+ \to \tau\nu$, $D^+ \to \tau\nu$, the LEP direct search, and other low energy constraints, as well as the branching ratio plots and discussion of LHC search prospects have been published in Ref. [29].

2.1 The Model

The Lepton-Specific Two Higgs Doublet Model follows the same framework as the Type-I and Type-II Two Higgs Doublet Models. We begin with two complex SU(2)-doublet fields

$$\Phi_l = \begin{pmatrix} \phi_l^+ \\ \frac{1}{\sqrt{2}}\left(\phi_l^{0,r} + v_l + i\phi_l^{0,i}\right) \end{pmatrix}, \qquad \Phi_q = \begin{pmatrix} \phi_q^+ \\ \frac{1}{\sqrt{2}}\left(\phi_q^{0,r} + v_q + i\phi_q^{0,i}\right) \end{pmatrix}, \tag{2.1}$$

and impose a symmetry under which the doublets transform as

$$\Phi_l \to -\Phi_l, \qquad \Phi_q \to \Phi_q, \qquad \ell_{Ri} \to -\ell_{Ri}.$$

Imposing this symmetry constrains the interaction behaviour of the theory. In order for the Lagrangian to remain invariant, leptons and quarks can not acquire mass from the same doublet, and leptons can become massive only by coupling to Φ_l.

This symmetry determines the most general Lagrangian allowed by the model. In the 2HDM-L, the full Lagrangian takes the form

$$\mathcal{L} = \mathcal{L}_{Kinetic} - V_{Scalar} + \mathcal{L}_{Yukawa}, \tag{2.2}$$

where

$$\mathcal{L}_{Yukawa} = -\sum_i \sum_j \left[y^u_{ij} \overline{u}_{Ri} \widetilde{\Phi}^\dagger_q Q_{Lj} + y^d_{ij} \overline{d}_{Ri} \Phi^\dagger_q Q_{Lj} + y^e_{ij} \overline{\ell}_{Ri} \Phi^\dagger_l L_{Lj} \right] + h.c, \quad (2.3)$$

$$\begin{aligned} V_{Scalar} = {} & m^2_{11} \Phi^\dagger_l \Phi_l + m^2_{22} \Phi^\dagger_q \Phi_q - \left(m^2_{12} \Phi^\dagger_l \Phi_q + h.c. \right) + \frac{\lambda_1}{2} \left(\Phi^\dagger_l \Phi_l \right)^2 \\ & + \frac{\lambda_2}{2} \left(\Phi^\dagger_q \Phi_q \right)^2 + \lambda_3 \left(\Phi^\dagger_l \Phi_l \right) \left(\Phi^\dagger_q \Phi_q \right) + \lambda_4 \left(\Phi^\dagger_q \Phi_l \right) \left(\Phi^\dagger_l \Phi_q \right) \\ & + \left[\frac{\lambda_5}{2} \left(\Phi^\dagger_l \Phi_q \right)^2 + h.c. \right], \end{aligned} \quad (2.4)$$

$$\mathcal{L}_{Kinetic} = |\mathcal{D}_\mu \Phi_l|^2 + |\mathcal{D}_\mu \Phi_q|^2. \quad (2.5)$$

In the above $\mathcal{D}_\mu$is the SM covariant derivative as given in Eq. 1.21.

As predicted from the imposed symmetry, one can see from $\mathcal{L}_{Yukawa}$ that Φ_l gives mass to leptons while Φ_q gives mass to both up and down type quarks. This model is analogous to the 2HDM-I in the quark sector, while when comparing the couplings of the up-type quarks to the leptons one recovers the relation of the 2HDM-II.

In any 2HDM, one has 5 physical Higgs states and another 3 unphysical states (the Goldstone bosons) which give mass to the gauge bosons. These states comprise the scalar fields that make up the Higgs doublets. The convention used is as follows

$$
\begin{aligned}
\phi_l^{0,i} &= G^0\cos(\beta) - A^0\sin(\beta) \\
\phi_q^{0,i} &= G^0\sin(\beta) + A^0\cos(\beta)
\end{aligned}
$$

$$
\begin{aligned}
\phi_l^{0,r} &= H^0\cos(\alpha) - h^0\sin(\alpha) \\
\phi_q^{0,r} &= H^0\sin(\alpha) + h^0\cos(\alpha)
\end{aligned}
$$

$$
\begin{aligned}
\phi_l^{\pm} &= G^{\pm}\cos(\beta) - H^{\pm}\sin(\beta) \\
\phi_q^{\pm} &= G^{\pm}\sin(\beta) + H^{\pm}\cos(\beta).
\end{aligned} \tag{2.6}
$$

Here β is once again the mixing angle that diagonalizes the mass matrices for the CP-odd and charged states, and α rotates between the gauge and mass basis of the CP-even states. This will be furthur discussed in Sec. 2.1.1.

As in the conventional two Higgs doublet models, the 2HDM-L defines a free parameter

$$\tan\beta \equiv \frac{v_q}{v_l}, \tag{2.7}$$

where v_l and v_q are the vevs of Φ_l and Φ_q respectively. From Sec. 1.4 we know these vevs are related to that of the Standard Model through the equation

$$\sqrt{v_l^2 + v_q^2} = v_{SM} \approx 246 \text{ GeV}. \tag{2.8}$$

Using this equation along with the definition of $\tan\beta$ one can also define the relations

$$\sin\beta = \frac{v_q}{v_{SM}}, \qquad \cos\beta = \frac{v_l}{v_{SM}}, \tag{2.9}$$

which become important for simplifying Feynman rules and masses.

2.1.1 Diagonalizing Mass Matrices - Scalar Field Theory

To illustrate the process of diagonalizing mass matrices and the outcome, I will give a brief outline for a scalar field theory with multiple particles. The most general Lagrangian which can be written for N scalar particles is [5]

$$\mathcal{L} = \frac{1}{2} I_{ij} \partial_\mu \phi^i \partial^\mu \phi^j - \frac{1}{2} \Gamma_{ij} \phi^i \phi^j, \tag{2.10}$$

where I_{ij} is the unit matrix and Γ_{ij} is an arbitrary real matrix.

Clearly from the implied summation over indices, there are terms such as $-\frac{1}{2}\Gamma_{12}\phi^1\phi^2$ which are not the conventional mass terms we are used to. Ideally it would be possible to have all fields decouple from one another so that the mass terms could be easily read off and each particle would satisfy its own equation of motion, the Klein-Gordon equation,

$$(-\partial^\mu \partial_\mu \phi + m^2 \phi) = 0. \tag{2.11}$$

We know we are always free to make a linear transformation of the fields ϕ^i, ϕ^j, as long as Eq. 2.10 remains quadratic in the new fields. Recall also that it is possible to diagonalize a real symmetric matrix by multiplying it on either side by an appropriate

orthogonal matrix such that

$$\mathcal{O}^T A_{ij} \mathcal{O} = \begin{pmatrix} a_1 & & & & \\ & a_2 & & & \\ & & . & & \\ & & & . & \\ & & & & a_n \end{pmatrix} \tag{2.12}$$

Defining $\phi^i = (\mathcal{O}\phi')^i$ and substituting this relation into Eq. 2.10, the scalar Lagrangian now reads

$$\mathcal{L} = \frac{1}{2}\partial^\mu \phi'^i \partial_\mu \phi'^i - \frac{1}{2}\Gamma'_{ij}\phi'^i\phi'^j, \tag{2.13}$$

with $\Gamma'_{ij} = (\mathcal{O}^T \Gamma \mathcal{O})_{ij}$. It is important to note that the term $\frac{1}{2}\partial^\mu \phi'^i \partial_\mu \phi'^i$ only contains one type of field since $(\mathcal{O}^T I \mathcal{O})_{ij} = I_{ij}$ for every orthogonal matrix $\mathcal{O}$. For the identity matrix the only non-zero entries are along the diagonal which restricts the first term to be quadratic in a single field with a coefficient of one.

Also note that from Eq. 2.12 it is apparent the matrix Γ'_{ij} is now diagonal with entries $\gamma_1, \gamma_2, \ldots, \gamma_n$. Each entry γ_i is the mass squared of the particle associated with field ϕ'^i. Since Γ'_{ij} is diagonal, all off diagonal entries are zero and there are no terms which couple two different fields.

By defining $\phi^i = (\mathcal{O}\phi')^i$, all fields have decoupled from one another. They now each satisfy their own equation,

$$(-\partial^\mu \partial_\mu + \gamma_i)\phi'^i = 0, \tag{2.14}$$

which was the desired result.

2.1.2 Mass Matrices - Lepton-Specific Two Higgs Doublet Model

In two Higgs doublet models it is common to work with a set of free parameters for a given theory. The parameters we would like to work with are λ_i and m_{12}^2. In order to find the masses of the Higgs particles in terms of these parameters we must first minimize the scalar potential with respect to the vev's and solve for m_{11}^2 and m_{22}^2. The result will be these masses in terms of the desired parameters. To begin we start with the usual scalar potential (see Eq. 2.4) and insert the vacuum expectation value $\langle \Phi_i \rangle = \frac{1}{\sqrt{2}} \begin{pmatrix} 0 \\ v_i \end{pmatrix}$. This again gives us the scalar potential

$$\begin{aligned} V_{scalar} &= \frac{1}{2}m_{11}^2 v_l^2 + \frac{1}{2}m_{22}^2 v_q^2 - m_{12}^2 v_l v_q + \frac{1}{8}\lambda_1 v_l^4 + \frac{1}{8}\lambda_2 v_q^4 \\ &\quad + \frac{1}{4}\lambda_3 v_l^2 v_q^2 + \frac{1}{4}\lambda_4 v_l^2 v_q^2 + \frac{1}{4}\lambda_5 v_l^2 v_q^2. \end{aligned} \tag{2.15}$$

except now it is in terms only of constants and parameters of the theory. Next we minimize V_{scalar} by differentiating with respect to v_l and v_q separately and setting each to zero. This gives two equations

$$\frac{\partial V}{\partial v_l} = m_{11}^2 v_l - m_{12}^2 v_q + \frac{1}{2}\lambda_1 v_l^3 + \frac{1}{2}v_l v_q^2 (\lambda_3 + \lambda_4 + \lambda_5) = 0, \tag{2.16}$$

$$\frac{\partial V}{\partial v_q} = m_{22}^2 v_q - m_{12}^2 v_l + \frac{1}{2}\lambda_2 v_q^3 + \frac{1}{2}v_l^2 v_q (\lambda_3 + \lambda_4 + \lambda_5) = 0, \tag{2.17}$$

which upon re-arranging give the relations for m_{11}^2 and m_{22}^2,

$$m_{11}^2 = m_{12}^2 \tan\beta - \frac{1}{2}\lambda_1 v_l^2 - \frac{1}{2}\left(\lambda_3 + \lambda_4 + \lambda_5\right) v_q^2 \tag{2.18}$$

$$m_{22}^2 = m_{12}^2 \cot\beta - \frac{1}{2}\lambda_2 v_q^2 - \frac{1}{2}\left(\lambda_3 + \lambda_4 + \lambda_5\right) v_l^2 \tag{2.19}$$

which are only in terms of m_{12}^2 and the λ_i parameters. Now we are ready to find the mass matrices and mass eigenstates.

2.1.21. CP-odd States

We begin with the piece of the scalar potential quadratic in those states that are negative under parity. This is given by

$$\begin{aligned} V &= \left(\phi_\ell^{0,i}\right)^2 \left\{\frac{1}{2}m_{11}^2 + \frac{1}{4}v_l^2\lambda_1 + \frac{1}{4}v_q^2\left(\lambda_3 + \lambda_4 - \lambda_5\right)\right\} \\ &+ \left(\phi_q^{0,i}\right)^2 \left\{\frac{1}{2}m_{22}^2 + \frac{1}{4}v_q^2\lambda_2 + \frac{1}{4}v_l^2\left(\lambda_3 + \lambda_4 - \lambda_5\right)\right\} \\ &+ \left(\phi_\ell^{0,i}\phi_q^{0,i}\right)\left\{v_l v_q \lambda_5 - m_{12}^2\right\} \end{aligned}$$

where all other fields have been ignored for simplicity of the calculation. By using the explicit form of the masses defined in Eqs. 2.18, 2.19, one can eliminate m_{11}^2 and m_{22}^2 in favor of m_{12}^2 giving

$$\begin{aligned} V &= \left(\phi_\ell^{0,i}\right)^2 \left\{\frac{m_{12}^2\tan\beta}{2} - \frac{\lambda_5 v_q^2}{2}\right\} \\ &+ \left(\phi_q^{0,i}\right)^2 \left\{\frac{m_{12}^2\cot\beta}{2} - \frac{\lambda_5 v_l^2}{2}\right\} \\ &+ \left(\phi_\ell^{0,i}\phi_q^{0,i}\right)\left\{v_l v_q \lambda_5 - m_{12}^2\right\}. \end{aligned}$$

The final step is to insert the form of $\phi_\ell^{0,i}$ and $\phi_q^{0,i}$ defined in Eq. 2.6. The result is that all cross terms involving A^0G^0 cancel leaving a mass term for A^0, $V = \frac{1}{2}m_{A^0}^2 A^0 A^0$ with

$$m_{A^0}^2 = (m_{12}^2 \tan\beta - \lambda_5 v_q^2)\csc^2\beta. \tag{2.20}$$

2.1.22. Charged Higgs States

Following the same process as for the CP-odd states, we write the scalar potential in terms only of charged fields such that

$$\begin{aligned} V &= \phi_\ell^- \phi_\ell^+ \left\{ m_{11}^2 + \frac{1}{2}\lambda_1 v_l^2 + \frac{1}{2}\lambda_3 v_q^2 \right\} \\ &+ \phi_q^- \phi_q^+ \left\{ m_{22}^2 + \frac{1}{2}\lambda_2 v_q^2 + \frac{1}{2}\lambda_3 v_l^2 \right\} \\ &+ \phi_\ell^- \phi_q^+ \left\{ \frac{1}{2} v_l v_q \lambda_4 + \frac{1}{2} v_l v_q \lambda_5 - m_{12}^2 \right\} \\ &+ \phi_\ell^+ \phi_q^- \left\{ \frac{1}{2} v_l v_q \lambda_4 + \frac{1}{2} v_l v_q \lambda_5 - m_{12}^2 \right\}. \end{aligned}$$

Once again substituting the form of $\phi_\ell^\pm$ and $\phi_q^\pm$ in terms of $H^\pm$ and $G^\pm$ from Eq. 2.6 and using the constraint of m_{11}^2 and m_{22}^2 from Eqs. 2.18, 2.19 we find the mass of the charged Higgs bosons, $V = M_{H^\pm}^2 H^+ H^-$ with

$$M_{H^\pm} = \left[m_{12}^2 \tan\beta - \frac{1}{2} v_q^2 (\lambda_4 + \lambda_5) \right] \csc^2\beta \tag{2.21}$$

in terms of free parameters. It is possible to also express v_q in terms of the Standard Model vev and an angle involving β (Eq. 2.9), however, since there are so many free parameters in the leptonic two Higgs doublet model, it is not beneficial to do so.

2.1.23. CP-even States

The CP-even states are the most complicated since they are linear combinations of two physical Higgs states. As with the CP-odd and charged states we write the scalar potential as

$$\begin{aligned} V &= \left(\phi_\ell^{0,r}\right)^2 \left[\frac{1}{2}m_{11}^2 + \frac{3}{4}\lambda_1 v_l^2 + \frac{1}{4}v_q^2\left(\lambda_3+\lambda_4+\lambda_5\right)\right] \\ &+ \left(\phi_q^{0,r}\right)^2 \left[\frac{1}{2}m_{22}^2 + \frac{3}{4}\lambda_2 v_q^2 + \frac{1}{4}v_l^2\left(\lambda_3+\lambda_4+\lambda_5\right)\right] \\ &+ \left(\phi_\ell^{0,r}\phi_q^{0,r}\right)\left[v_l v_q\left(\lambda_3+\lambda_4+\lambda_5\right) - m_{12}^2\right]. \end{aligned}$$

Using Eq. 2.18 and Eq. 2.19 to eliminate m_{11}^2 and m_{22}^2 and write

$$\begin{aligned} V &= \left(\phi_\ell^{0,r}\right)^2 \left[\frac{1}{2}m_{12}^2\tan^2\beta + \frac{1}{2}\lambda_1 v_l^2\right] \\ &+ \left(\phi_q^{0,r}\right)^2 \left[\frac{1}{2}m_{12}^2\cot^2\beta + \frac{1}{2}\lambda_2 v_q^2\right] \\ &+ \left(\phi_\ell^{0,r}\phi_q^{0,r}\right)\left[v_l v_q\left(\lambda_3+\lambda_4+\lambda_5\right) - m_{12}^2\right], \end{aligned}$$

we can write a term for the CP-even masses, $V = \frac{1}{2}\phi_i^{0,r} M_{ij}^2 \phi_j^{0,r}$ with the squared mass matrix,

$$M^2 = \begin{pmatrix} M_{11}^2 & M_{12}^2 \\ M_{21}^2 & M_{22}^2 \end{pmatrix}, \tag{2.22}$$

where

$$M_{11}^2 = m_{12}^2\tan^2\beta + \lambda_1 v_l^2 \tag{2.23}$$

$$M_{22}^2 = m_{12}^2\cot^2\beta + \lambda_2 v_q^2 \tag{2.24}$$

$$M_{12}^2 = M_{21}^2 = v_l v_q\left(\lambda_3+\lambda_4+\lambda_5\right) - m_{12}^2. \tag{2.25}$$

As is clear from the definition of $\phi_i^{0,r}$ in Eq. 2.6, α is the angle which diagonalizes the mass matrix of Eq. 2.22 and rotates between the gauge and mass basis.

2.1.3 Feynman Rules

To determine the Feynman rules one can substitute the explicit form of the fields into the full Lagrangian and extract the relevant couplings. For the scope of this thesis we will mainly be interested in the couplings of the charged Higgs to fermions. These couplings are straightforward for leptons since we have assumed that neutrinos are massless and therefore can not mix between generations. The quarks however are able to change generations through the CKM matrix as they do in the SM.

2.1.31. Yukawa Lagrangian and the CKM Matrix

In the Standard Model the Cabibbo–Kobayashi–Maskawa (CKM) matrix arises from diagonalizing the up-type and down-type quark mass matrices seperately. The CKM matrix appears in the fermion sector of the 2HDM-L through the same process, which is outlined below. The quark piece of the Yukawa Lagrangian for the lepton-specific two Higgs doublet model is

$$\mathcal{L}_{Yukawa}^{quark} = -\sum_{i=1}^{3}\sum_{j=1}^{3}\left[y_{ij}^{u}\overline{u}_{Ri}\tilde{\Phi}_q^{\dagger}Q_{Lj} + y_{ij}^{d}\bar{d}_{Ri}\Phi_q^{\dagger}Q_{Lj}\right] + h.c. \tag{2.26}$$

In order to find the coupling of the charged Higgs particles to fermions one can take the explicit form of the scalar fields, $\phi_l^{\pm} = G^{\pm}\cos\beta - H^{\pm}\sin\beta$, $\phi_q^{\pm} = G^{\pm}\sin\beta + H^{\pm}\cos\beta$, and extract only those terms relevant to the coupling of charged Higgs bosons. Inserting the proportionalities $\tilde{\Phi}_q^{\dagger}Q_{Lj} \propto -\cos\beta d_{Lj}H^{+}$, $\Phi_q^{\dagger}Q_{Lj} \propto \cos\beta u_{Lj}H^{-}$

into Eq. 2.26 we find

$$\mathcal{L}^{quark}_{Yukawa} = -\sum_{i=1}^{3}\sum_{j=1}^{3}\left[-y^u_{ij}\overline{u}_{Ri}d_{Lj}H^+\cos\beta + y^d_{ij}\bar{d}_{Ri}u_{Lj}H^-\cos\beta\right] + h.c. \tag{2.27}$$

The next step is to find the quark mass matrices in terms of the Yukawa couplings. This is done by returning to Eq. 2.26 and setting all fields in the Higgs doublet to zero. By including only the vev it is possible to solve for the fermion masses writing

$$\begin{aligned}
\mathcal{L}^{quark}_{Yukawa} &= -\sum_{i=1}^{3}\sum_{j=1}^{3}\frac{1}{\sqrt{2}}\left[y^u_{ij}\overline{u}_{Ri}v_q u_{Lj} + y^d_{ij}\bar{d}_{Ri}v_q d_{Lj}\right] + h.c. \\
&= -\sum_{i=1}^{3}\sum_{j=1}^{3}\frac{1}{\sqrt{2}}\left[y^u_{ij}v_q\overline{u}_i P_L u_j + y^d_{ij}v_q\bar{d}_i P_L d_j + y^u_{ij}v_q\overline{u}_i P_R u_j + y^d_{ij}v_q\bar{d}_i P_R d_j\right] \\
&= -\sum_{i=1}^{3}\sum_{j=1}^{3}\frac{1}{\sqrt{2}}\left[y^u_{ij}v_q\overline{u}_i u_j + y^d_{ij}v_q\bar{d}_i d_j\right] \qquad (2.28) \\
&= -\sum_{i=1}^{3}\sum_{j=1}^{3} M^u_{ij}\overline{u}_i u_j + M^d_{ij}\bar{d}_i d_j \qquad (2.29)
\end{aligned}$$

and substituting $v_q = v_{SM}\sin\beta = \frac{2M_W}{g}\sin\beta$ from Eq. 2.9 gives $M^{u,d}_{ij} = \frac{\sqrt{2}M_W}{g}y^{u,d}_{ij}\sin\beta$. Re-arranging for the Yukawa couplings in terms of the mass matrices

$$y^d_{ij} = \frac{gM^d_{ij}}{\sqrt{2}M_W}\csc\beta, \qquad y^u_{ij} = \frac{gM^u_{ij}}{\sqrt{2}M_W}\csc\beta, \tag{2.30}$$

and upon substituting Eq. 2.30 into Eq. 2.27 gives

$$\mathcal{L}^{quark}_{Yukawa} = -\sum_{i=1}^{3}\sum_{j=1}^{3}\frac{g}{\sqrt{2}M_W}\left[-M^u_{ij}\overline{u}_{Ri}d_{Lj}H^+\cot\beta + M^d_{ij}\bar{d}_{Ri}u_{Lj}H^-\cot\beta\right] + h.c. \tag{2.31}$$

The quark terms in the above equations are written in the gauge basis. As seen in subsection 2.1.1, diagonalizing a real symmetric mass matrix is possible by multiplying it with an orthogonal transformation on the left and right. In the SM, the quark mass matrices are complex and in general not Hermitian so it is necessary to diagonalize

these matrices by rotating the left- and right-handed up-type quarks and down-type quarks by 4 separate unitary matrices

$$\begin{pmatrix} u_1 \\ u_2 \\ u_3 \end{pmatrix}_{L,R} = U_{L,R} \begin{pmatrix} u \\ c \\ t \end{pmatrix}_{L,R} \quad \text{and} \quad \begin{pmatrix} d_1 \\ d_2 \\ d_3 \end{pmatrix}_{L,R} = D_{L,R} \begin{pmatrix} d \\ s \\ b \end{pmatrix}_{L,R} . \tag{2.32}$$

After diagonalizing the mass matrices a new matrix appears in the Yukawa Lagrangian from the combination $U_L^\dagger D_L = V$. The CKM matrix, V_{ij}, shows up in the the quark section of the Yukawa Lagrangian as

$$\mathcal{L}_{Yukawa}^{quark} = -\sum_{i=1}^{3}\sum_{j=1}^{3} \frac{g}{\sqrt{2}M_W} \left[-m_{ui} V_{ij} \bar{u}_i P_L d_j H^+ \cot\beta + m_{dj} V_{ij}^* \bar{d}_j P_L u_i H^- \cot\beta \right] + h.c. \tag{2.33}$$

where the mass matrices of the up-type and down-type quarks are replaced by the appropriate mass eigenvalues and the quark terms in the above expression are now written in the quark mass basis. The lepton Yukawa Lagrangian takes a similar form, however, under the assumption of massless neutrinos an analogous mixing matrix does not appear in the lepton sector. The lepton Yukawa Lagrangian is written as

$$\mathcal{L}_{Yukawa}^{lepton} = -\sum_{i=1}^{3} \frac{g}{\sqrt{2}M_W} \left[M_i^\ell \bar{\ell}_i P_L \nu_i H^+ \tan\beta \right] + h.c. \tag{2.34}$$

and from Eq. 2.33 and Eq. 2.34 the Feynman rules in the quark mass basis can be read off as

$$H^+ \bar{u}_i d_j \;:\; \frac{ig}{\sqrt{2}M_W} V_{ij} \cot\beta \left(m_{ui} P_L - m_{dj} P_R \right), \tag{2.35}$$

$$H^+ \bar{\ell}_k \nu_{\ell k} \;:\; \frac{ig}{\sqrt{2}M_W} m_{\ell k} \tan\beta P_L, \tag{2.36}$$

where m_{ui}, m_{dj}, $m_{\ell k}$ are the masses of the specific particle with the generation denoted by the subscript. Equation 2.35 shows that the quark couplings are proportional to $\cot\beta$, while from Eq. 2.36 one can see the lepton couplings are proportional to $\tan\beta$.

2.1.4 Perturbativity of the τ Yukawa Coupling

By rearranging Eq. 2.9 and substituting the expression for v_l into the tau Yukawa coupling y_τ one can set an allowed range for $\tan\beta$ based on perturbativity constraints. In the 2HDM-L, perturbativity of the tau Yukawa coupling,

$$y_\tau = \frac{\sqrt{2}m_\tau}{v_\ell} = \frac{\sqrt{2}m_\tau}{v_{SM}\cos\beta}, \tag{2.37}$$

gives an upper bound on $\tan\beta$.

From Eqs. 2.7 and 2.9 we can see that for large $\tan\beta$ the vacuum expectation value associated with the leptons must be very small and leads to enhanced lepton couplings.

Higher order loop calculations give corrections proportional to y_i^2, and in order to make perturbation theory a valid approximation we must maintain that the correction is at most of order 1 relative to the leading order. The phase space integration of higher level processes includes a factor of $\frac{1}{(4\pi)^2}$, so we make the cut off $y_i \lesssim 4\pi$. From this we find y_τ can be approximated as

$$y_\tau \simeq \frac{\sqrt{2}m_\tau \tan\beta}{v_{SM}} \lesssim 4\pi$$

which leads to the upper bound

$$\tan\beta \lesssim 1228. \tag{2.38}$$

Clearly from the above constraint on $\tan\beta$, we can see that $\tan\beta$ values up to 100 or 200 are completely perturbative since they correspond to y_τ values of about 1 or 2, respectively.

2.2 Experimental Constraints

In this section the new experimental constraints are presented for the parameters $M_{H^\pm}$ and $\tan\beta$ in the lepton-specific 2HDM. These constraints are found by adapting search modes for other 2HDMs, or based on direct low-energy measurements. A lower bound of $M_{H^\pm} \geq 92.0$ GeV is found by adapting the OPAL charged Higgs search at LEP [30], there are two allowed mass ranges $0.61\tan\beta$ GeV $\leq M_{H^\pm} \leq 0.73\tan\beta$ GeV or $M_{H^\pm} \geq 1.4\tan\beta$ GeV from lepton universality in tau decay at the 95% confidence level, and there are other weaker constraints found from Michel parameters in muon and tau decay as well as other low-energy processes.

2.2.1 Limits from LEP-2 Direct Search

In 2000, four collaborations (ALEPH, DELPHI, L3, and OPAL) at LEP made a direct search for the charged Higgs boson predicted by the Type-II two Higgs doublet model. Combining their results they were able to place a lower bound on $M_{H^\pm}$ which varied with the allowed decay modes of $H^\pm$ [31].

Assuming a charged Higgs mass below about 170 GeV (which excludes the decay of $H^\pm$ to tb) the branching ratio (BR) of $H^+ \to \tau^+\nu_\tau$ already dominates at 94% for $\tan\beta = 3$ in the lepton-specific model. For our purposes we take $\tan\beta \geq 5$ and

assume that $BR(H^+ \to \tau^+\nu_\tau) \simeq 1$ for all considered values of $\tan\beta$. Details on $H^\pm$ decays will be presented in Sec. 2.3.

For $BR(H^+ \to \tau^+\nu_\tau) = 1$, the OPAL collaboration has found the lower bound [30]

$$M_{H^\pm} \geq 92.0 \text{ GeV}. \tag{2.39}$$

For the 2HDM-L we will thus exclude masses of the charged Higgs below 92.0 GeV.

2.2.2 Lepton Universality in Muon and Tau Decays

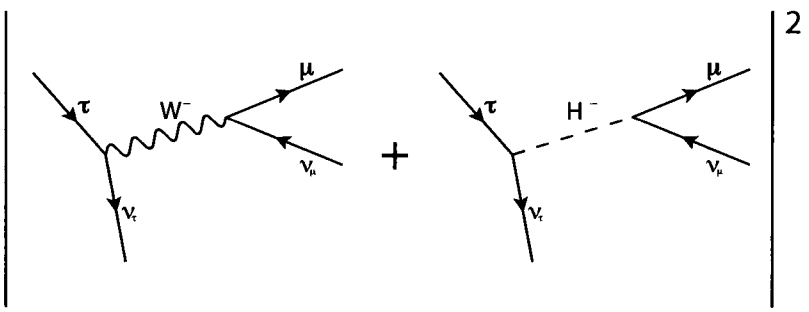

Figure 2.1: Diagrams of τ decay via W bosons (left) and $H^\pm$ bosons (right).

In the Standard Model charged leptons decay through one channel mediated by a $W^\pm$ boson (first diagram in Fig. 2.1). In a general 2HDM, charged leptons can also decay through the exchange of a charged Higgs boson (second diagram in Fig. 2.1). Decays of charged leptons are of special interest in the 2HDM-L since there will be an enhancement of $\tan^2\beta$ in the amplitude due to the fact that both couplings of $H^\pm$ are to leptons. As well the perturbativity of y_τ allows large values of $\tan\beta$ which when increased gives a more competitive contribution to the total width from the charged

Higgs exchange.

The decay of the muon has only one final state which is predetermined by the mass of the initial particle and conservation laws; however the tau lepton is able to decay to either the muon or electron with their associated neutrinos. The partial width including charged Higgs exchange for these leptonic decays is given by [32, 33]

$$\Gamma\left(L \to l\overline{\nu_l}\nu_L\right) = \frac{G_F^2 m_L^5}{192\pi^3}\left[\left(1+\frac{3}{5}\frac{m_L^2}{m_W^2}\right)f(m_l^2/m_L^2) + \frac{1}{4}m_\ell^2 m_L^2 \frac{\tan^4\beta}{M_{H^+}^4} f(m_l^2/m_L^2) - 2m_\ell^2 \frac{\tan^2\beta}{M_{H^+}^2} g(m_l^2/m_L^2)\right] \tag{2.40}$$

where G_F is the Fermi constant, L denotes the initial lepton, ℓ denotes the final state lepton and the phase space factors f and g are given by [33]

$$f(x) = 1-8x+8x^3-x^4-12x^2\ln x, \qquad g(x) = 1+9x-9x^2-x^3+6x(1+x)\ln x. \tag{2.41}$$

The first term in the square brackets of Eq. 2.40 is the contribution to the total width from W exchange, the second term is the contribution from $H^\pm$ exchange, and the third term is the destructive interference term which comes from a combination of the W and $H^\pm$diagrams. The factor $1+\frac{3}{5}\frac{m_L^2}{m_W^2}$ in the first term comes from the momentum integration of the Feynman rule for the W propagator and we acknowledge that the integration over momentum to give the second and third terms would have terms of the form $1+\frac{m_L^2}{M_{H^\pm}^2}$. We have neglected these terms since the contribution to the total width from charged Higgs exchange is already small and this factor would be a tiny correction to an already small term.

It is possible to take the ratio of decaying charged leptons. Then, by experimentally measuring the ratio of the decay partial widths one can see if there is a discrepancy

between generations, and how much room there is for new physics.

We write the τ lifetime τ_τ in terms of the muon lifetime τ_μ as [34]

$$\begin{aligned}
\tau_\tau &= \tau_\mu \frac{g_\mu^2}{g_\tau^2}\frac{m_\mu^5}{m_\tau^5} BR\left(\tau \to e\overline{\nu}_e\nu_\tau\right)\frac{f\left(m_e^2/m_\mu^2\right) r_{RC}^\mu}{f\left(m_e^2/m_\tau^2\right) r_{RC}^\tau}, \\
\tau_\tau &= \tau_\mu \frac{g_e^2}{g_\tau^2}\frac{m_\mu^5}{m_\tau^5} BR\left(\tau \to \mu\overline{\nu}_\mu\nu_\tau\right)\frac{f\left(m_e^2/m_\tau^2\right) r_{RC}^\mu}{f\left(m_\mu^2/m_\tau^2\right) r_{RC}^\tau}.
\end{aligned} \tag{2.42}$$

Here g_e, g_μ, and g_τ are effective charged current couplings that parametrize deviations from their SM value of 1 which arise from a bias in flavour universality from Higgs exchange. Referring back to Eq. 2.40, g_e, g_μ, and g_τ contain the terms in the square brackets. In Eq. 2.42 $f\left(m_i^2/m_j^2\right)$ is a phase space factor to account for the nonzero final state lepton masses (given in Eq. 2.41), and r_{RC}^i are QED radiative corrections. To date, the most precise measurements made of the ratio of these effective couplings are [34]

$$\frac{g_\mu}{g_\tau} = 0.9982 \pm 0.0021, \tag{2.43}$$

$$\frac{g_\mu}{g_e} = 0.9999 \pm 0.0020. \tag{2.44}$$

The observable g_μ/g_e comes from the ratio of the BRs of $\tau \to \mu\nu\nu$ vs. $\tau \to e\nu\nu$. In the 2HDM-L we find,

$$\frac{g_\mu^2}{g_e^2} = \frac{(1+3m_\tau^2/5M_W^2) + m_\mu^2 m_\tau^2 \tan^4\beta/4M_{H^\pm}^4 - (2m_\mu^2\tan^2\beta/M_{H^\pm}^2) g(m_\mu^2/m_\tau^2)/f(m_\mu^2/m_\tau^2)}{(1+3m_\tau^2/5M_W^2) + m_e^2 m_\tau^2 \tan^4\beta/4M_{H^\pm}^4 - (2m_e^2\tan^2\beta/M_{H^\pm}^2) g(m_e^2/m_\tau^2)/f(m_e^2/m_\tau^2)}. \tag{2.45}$$

The square root of this ratio is plotted in Fig. 2.2 as a function of $M_{H^\pm}/\tan\beta$, along with the current 2σ experimental limits from Ref. [34]. One would expect $g_\mu/g_e \geq 1$ since the muon mass is much larger than that of the electron. However, as the ratio $M_{H^\pm}/\tan\beta$ approaches 1, the interference term contributes more which gives the

unexpected decrease of the ratio g_μ/g_e in Fig. 2.2. Inserting the experimental results yields two allowed regions at 95% CL:

$$0.61 \tan\beta \text{ GeV} \leq M_{H^\pm} \leq 0.73 \tan\beta \text{ GeV} \qquad \text{or} \qquad M_{H^\pm} \geq 1.4 \tan\beta \text{ GeV}. \quad (2.46)$$

This constraint begins to exclude parameter regions beyond the LEP-II bound when $\tan\beta \gtrsim 65$. The observable g_μ/g_τ is not used to constrain this model since it corresponds to the ratio of the BR's of $\mu \to e\nu\nu$ vs. $\tau \to e\nu\nu$ which in the 2HDM-L gives

$$\frac{g_\mu^2}{g_\tau^2} = \frac{(1 + 3m_\mu^2/5M_W^2) + m_\mu^2 m_e^2 \tan^4\beta/4M_{H^\pm}^4 - (2m_e^2 \tan^2\beta/M_{H^\pm}^2) g(m_e^2/m_\mu^2)/f(m_e^2/m_\mu^2)}{(1 + 3m_\tau^2/5M_W^2) + m_e^2 m_\tau^2 \tan^4\beta/4M_{H^\pm}^4 - (2m_e^2 \tan^2\beta/M_{H^\pm}^2) g(m_e^2/m_\tau^2)/f(m_e^2/m_\tau^2)}. \quad (2.47)$$

One can see from Eq. 2.47 that the m_e^2 dependence of the interference and charged Higgs exchange terms will only allow this observable to deviate slightly from its SM value of 1 and therefore only weakly constrain the parameter $M_{H^\pm}$.

At the proposed SuperB high-luminosity flavour factory [35], we should expect to see g_μ/g_e measured to better than 0.05% [34]. Assuming the central value is consistent with the SM this would give an even tighter constraint on the charged Higgs mass,

$$0.64 \tan\beta \text{ GeV} \leq M_{H^\pm} \leq 0.67 \tan\beta \text{ GeV} \qquad \text{or} \qquad M_{H^\pm} \geq 3.2 \tan\beta \text{ GeV}. \quad (2.48)$$

Such a constraint would exclude parameter regions beyond the LEP-II bound when $\tan\beta \gtrsim 30$.

The constraints on $M_{H^\pm}$ and $\tan\beta$ due to LEP-II direct searches and flavour universality in τ decays are summarized in Fig. 2.3.

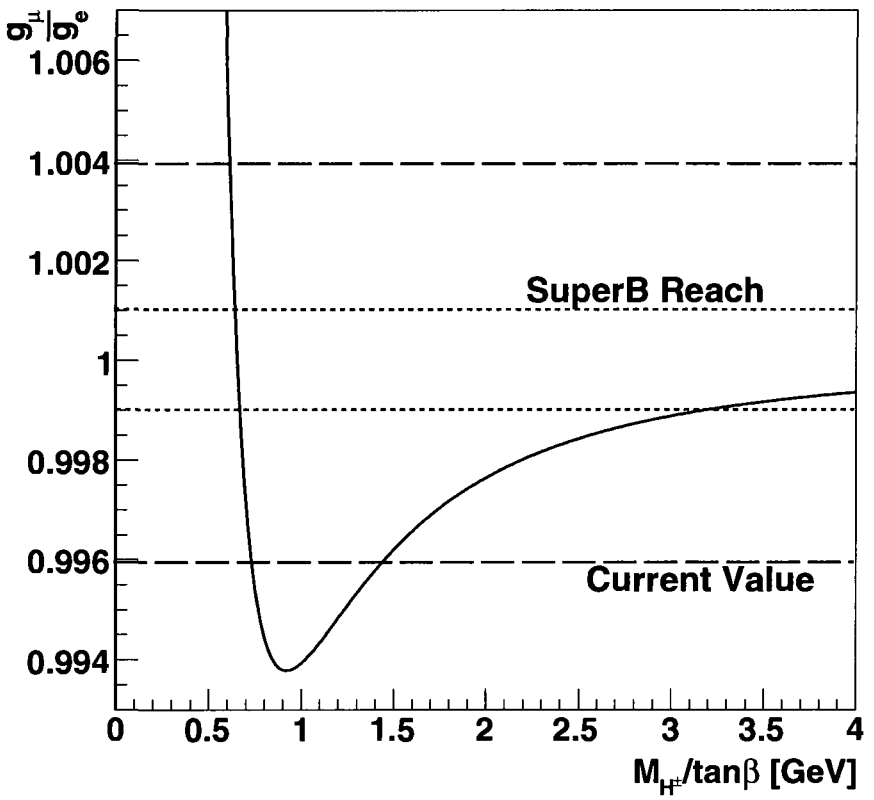

Figure 2.2: Prediction for g_μ/g_e in the lepton-specific 2HDM as a function of $M_{H^\pm}/\tan\beta$ (solid line). Horizontal dashed lines indicate the current 2σ allowed range from lepton universality in τ decays (outer lines) and the future anticipated reach of SuperB (inner lines).

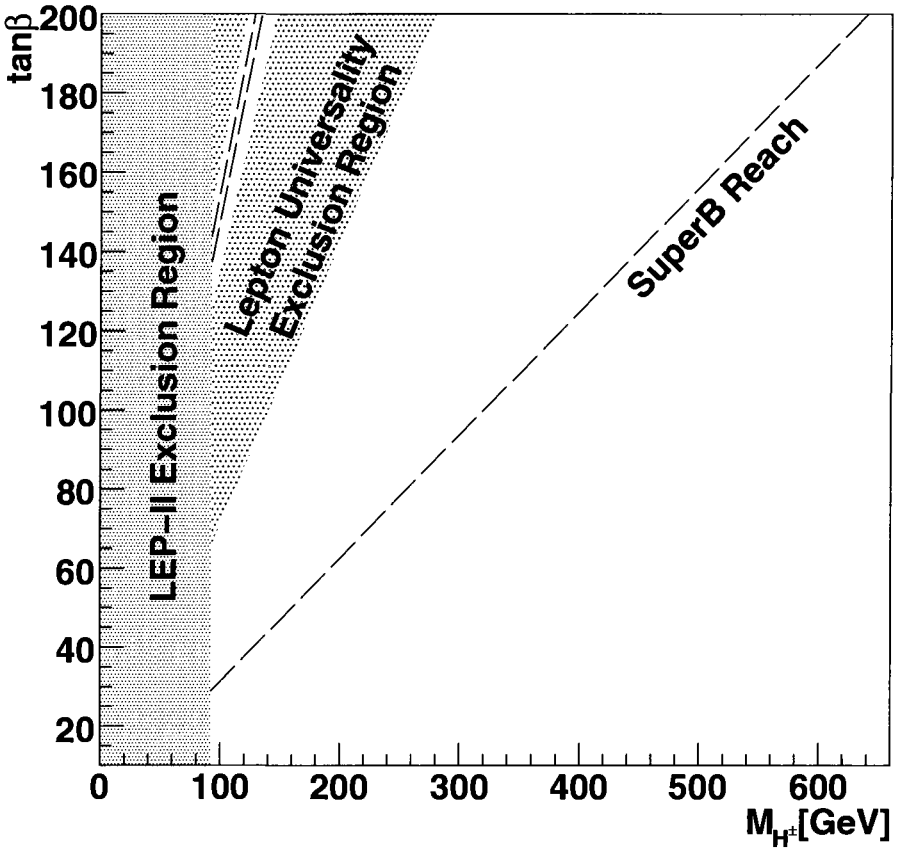

Figure 2.3: Constraints on the $\tan\beta - M_{H^\pm}$ plane at the 95% C.L.

2.2.3 Michel Parameters in Muon and Tau Decay

The Michel parameters are a way to express the energy and angular distribution of daughter leptons (e or μ from τ decay) emitted by decaying polarized charged leptons. One can write the differential decay rate of the given charged lepton in terms of four parameters, [36]ρ, ξ, δ, and η. These are constants in the SM with values $\rho = \frac{3}{4}$, $\xi = 1$, $\eta = 0$, and $\delta = \frac{3}{4}$. The differential decay rate for the decay of

muons or tau leptons is given by [37]

$$\frac{d^2\Gamma}{dx\, d\cos\theta} \propto x^2 \left\{ 3(1-x) + \frac{2\rho}{3}(4x-3) + 3\eta x_0(1-x)/x \right. \\ \left. \pm \mathcal{P}_L \xi \cos\theta \left[1 - x + \frac{2\delta}{3}(4x-3) \right] \right\}, \tag{2.49}$$

where $\mathcal{P}_L$ is the polarization of the parent particle L , θ is the angle between the emitted daughter particle ℓ and the axis of polarization of the parent particle, and $x = 2E_\ell/m_L$, $x_0 = 2m_\ell/m_L$.

By writing the most general matrix element for charged lepton decay into leptons as the sum [38,39]

$$\mathcal{M} = 4\frac{G_F}{\sqrt{2}} \sum_{\gamma=S,V,T} \sum_{\alpha,\beta=R,L} g^\gamma_{\alpha\beta} \left\langle \bar{l}_\alpha \left| \Gamma^\gamma \right| (\nu_l) \right\rangle \left\langle (\bar{\nu}_L) \left| \Gamma_\gamma \right| L_\beta \right\rangle, \tag{2.50}$$

the coupling constants $g^\gamma_{\alpha\beta}$ can be read off from the expansion of terms in the matrix element. In Eq. 2.50, $\gamma = S$, V, or T denotes scalar ($\Gamma^S = 1$), vector ($\Gamma^V = \gamma^\mu$), or tensor ($\Gamma^T = \sigma^{\mu\nu}/\sqrt{2} = i[\gamma^\mu, \gamma^\nu]/2\sqrt{2}$) interactions, respectively, and the chiralities of ℓ and L are specified by α and β, respectively [40]. In the Standard Model the weak force is mediated by massive vector bosons which link the interactions of left handed particles. The behaviour of the weak interaction in the SM leaves only $g^V_{LL} = -\frac{1}{4}$ and all other coupling constants equal to zero. When we expand the Higgs sector of the SM to have two Higgs doublets as in the 2HDM-L, then it is possible to also have scalar interactions between right handed charged leptons mediated by charged Higgs bosons so the coupling constant g^S_{RR} must also be included.

The Michel parameters written in terms of all possible coupling constants are [41]

$$\begin{aligned}
\rho &= \frac{3}{4} - \frac{3}{4}\left[|g_{RL}^V|^2 + |g_{LR}^V|^2 + 2|g_{RL}^T|^2 + 2|g_{LR}^T|^2 + Re\left(g_{RL}^S g_{RL}^{T*} + g_{LR}^S g_{LR}^{T*}\right)\right], \\
\eta &= \frac{1}{2} Re\left[g_{RR}^V g_{LL}^{S*} + g_{LL}^V g_{RR}^{S*} + g_{RL}^V\left(g_{LR}^{S*} + 6g_{LR}^{T*}\right) + g_{LR}^V\left(g_{RL}^{S*} + 6g_{RL}^{T*}\right)\right], \\
\xi &= 1 - \frac{1}{2}|g_{LR}^S|^2 - \frac{1}{2}|g_{RR}^S|^2 - 4|g_{RL}^V|^2 + 2|g_{LR}^V|^2 - 2|g_{RR}^V|^2 \\
&\quad +2|g_{LR}^T|^2 - 8|g_{RL}^T|^2 + 4Re\left(g_{LR}^S g_{LR}^{T*} - g_{RL}^S g_{RL}^{T*}\right), \\
\xi\delta &= \frac{3}{4} - \frac{3}{8}|g_{RR}^S|^2 - \frac{3}{8}|g_{LR}^S|^2 - \frac{3}{2}|g_{RR}^V|^2 - \frac{3}{4}|g_{RL}^V|^2 - \frac{3}{4}|g_{LR}^V|^2 \\
&\quad -\frac{3}{2}|g_{RL}^T|^2 - 3|g_{LR}^T|^2 + \frac{3}{4}Re\left(g_{LR}^S g_{LR}^{T*} - g_{RL}^S g_{RL}^{T*}\right)
\end{aligned} \tag{2.51}$$

and including only g_{RR}^S and g_{LL}^V the Michel parameters in the 2HDM-L are

$$\begin{aligned}
\rho &= \frac{3}{4}, \\
\eta &= \frac{1}{2} Re\left[g_{LL}^V g_{RR}^{S*}\right], \\
\xi &= 1 - \frac{1}{2}|g_{RR}^S|^2, \\
\xi\delta &= \frac{3}{4} - \frac{3}{8}|g_{RR}^S|^2.
\end{aligned} \tag{2.52}$$

Expanding Eq. 2.50 for the specific case of muon decay or tau lepton decay in the 2HDM-L we find $g_{LL}^V = -\frac{1}{4}$ from SM W boson exchange, $g_{RR}^S = m_L m_\ell \tan^2\beta/4M_{H^\pm}^2$ from $H^\pm$ exchange and all other couplings equal to zero. Inserting these values into

Eq.2.52 the Standard Model Michel parameters are modified as follows:

$$\begin{aligned}
\rho &= \frac{3}{4}, \\
\eta &= -\frac{m_L m_\ell}{32}\frac{\tan^2\beta}{M_{H^\pm}^2}, \\
\xi &= 1 - \frac{m_L^2 m_\ell^2}{32}\frac{\tan^4\beta}{M_{H^\pm}^4}, \\
\xi\delta &= \frac{3}{4}\left[1 - \frac{m_L^2 m_\ell^2}{32}\frac{\tan^4\beta}{M_{H^\pm}^4}\right] = \frac{3}{4}\xi.
\end{aligned}$$

From the above set of equations we can see that ρ and δ are constant in the 2HDM-L and do not constrain the ratio $\frac{\tan\beta}{M_{H^\pm}}$. The constraints from Michel parameters in the 2HDM-L are summarized in Tab. 2.1 below. The strongest constraints come from parameters ξ and η in the decay of $\tau \to \mu\bar{\nu}_\mu\nu_\tau$; coincidentally they both yield

$$M_{H^\pm} \geq 0.34 \tan\beta \text{ GeV}, \tag{2.53}$$

which is weaker than the constraint from lepton universality.

Process	Observable	Constraint
$\mu \to e\bar{\nu}\nu$	$\eta = 0.001 \pm 0.024$	$M_{H^\pm} \geq 0.006 \tan\beta$ GeV
$\tau \to \mu\bar{\nu}\nu$	$\eta = 0.094 \pm 0.073$	$M_{H^\pm} \geq 0.34 \tan\beta$ GeV
	$\xi = 1.030 \pm 0.059$	$M_{H^\pm} \geq 0.34 \tan\beta$ GeV
$\tau \to e\bar{\nu}\nu$	$\xi = 0.994 \pm 0.040$	$M_{H^\pm} \geq 0.023 \tan\beta$ GeV

Table 2.1: Constraints on $M_{H^\pm}$ and $\tan\beta$ at 95% CL from the Michel parameters in muon and τ decay. The values given are world averages from Ref. [1]. No separate measurement of ξ in muon decay or of η in $\tau \to e\bar{\nu}\nu$ is quoted.

2.2.4 $B^+ \to \tau^+\nu_\tau$

In the Standard Model, the partial width for the decay $B^+ \to \tau^+\nu_\tau$ is given by

$$\Gamma_{\rm SM}(B^+ \to \tau^+\nu_\tau) = \frac{G_F^2}{8\pi} f_{B^+}^2 m_{B^+} m_\tau^2 |V_{ub}|^2 \left[1 - \frac{m_\tau^2}{m_{B^+}^2}\right]^2 . \tag{2.54}$$

The partial width is proportional to m_τ^2 because of helicity suppression (see Sec. 2.2.41.) and the term in the square brackets arises from the phase space. The dependence on m_l^2 from helicity suppression means the partial width is larger for heavier leptons, with τ giving the largest contribution.

2.2.41. Helicity Suppression

Demanding Lorentz invariance, the coupling of B^+ to W_μ^+ must be of the form $q_\mu f_{B^+}(q^2)$,where q_μ is the four-momentum of the meson and

$$i f_{B^+} q_\mu = \left\langle 0 \left| \bar{b}\gamma_\mu\gamma_5 u \right| B^+(p) \right\rangle \tag{2.55}$$

is the definition of the decay constant f_{B^+}. In the Standard Model the matrix element is

$$\mathcal{M} = \frac{ig^2}{8M_W^2} f_{B^+} q_\mu \left[\bar{u}(k')\gamma^\mu(1-\gamma_5)v(q')\right], \tag{2.56}$$

where k' (q') is the four-momentum of the final state neutrino (τ^+).

The m_τ^2 dependence of Eq. 2.54 arises from writing Eq. 2.56 as

$$\mathcal{M} = \frac{ig^2}{8M_W^2} f_{B^+} \left[\bar{u}(k')\not{q}(1-\gamma_5)v(q')\right] \tag{2.57}$$

and substituting $\bar{u}(k')\not{q} = \bar{u}(k')(\not{q}' + \not{k}')$. Using the identities from the Dirac equation,

$\not{q}v(q') = -m_\tau v(q')$, $\bar{u}(k')\not{k}' = 0$ and squaring the resulting matrix element gives

$$|\bar{\mathcal{M}}|^2 = \frac{g^4}{8M_W^4}|V_{ub}|f_{B^+}^2 m_\tau^2 (k' \cdot q'). \tag{2.58}$$

Using Fermi's golden rule [42],

$$d\Gamma = \frac{1}{2m_{B^+}} \frac{d^3q'}{2E(2\pi)^3} \frac{d^3k'}{2\omega(2\pi)^3} (2\pi)^4 \delta(m_{B^+} - E - \omega)\delta^3(\vec{q}' + \vec{k}')|\bar{\mathcal{M}}|^2, \tag{2.59}$$

where $E = q_0'$ and $\omega = k_0'$, and inserting Eq. 2.58 we find the result quoted in Eq. 2.54. The factor $(m_\tau/m_{B^+})^2$ is called a helicity suppression which arises from coupling fermions to a scalar meson imposing conservation of angular momentum.

The helicity of a particle is defined as $+1$ if the spin and linear momentum are aligned in parallel, and -1 if the spin and angular momentum are aligned in anti-parallel. The bound state B^+ has total angular momentum $J = 0$ which means that the neutrino and lepton which come out back to back must have opposite spins. This implies that for the neutrino and lepton to couple to the W, which couples to left-handed fermions, then the helicity of the lepton must flip and a factor of $(m_\tau/m_{B^+})^2$ must be introduced. This factor suppresses the partial width for $m_\tau \ll m_{B^+}$.

2.2.42. Allowed Ranges for M_{H^+} from $B^+ \to \tau^+\nu$

In the 2HDM-L, we need to calculate the charged Higgs diagram and interference term. In order to evaluate the diagram associated with charged Higgs exchange we need to start with Eq. 2.55 and find a way to extract an expression for $\langle 0|\bar{b}\gamma_5 u|B^+\rangle$. Taking Eq. 2.55 and multiplying each side by q^μ gives $\langle 0\,|\bar{b}\not{q}\gamma_5 u|\,B^+(p)\rangle = f_{B^+}m_{B^+}^2$. Then once again using the Dirac equation we find $(m_u - m_b)\langle 0|\bar{b}\gamma_5 u|B^+\rangle = f_{B^+}m_{B^+}^2$

or

$$\langle 0|\bar{b}\gamma_5 u|B^+\rangle = \frac{f_{B^+} m_{B^+}^2}{(m_u - m_b)}. \tag{2.60}$$

Neglecting the mass of the muon, the matrix element for the charged Higgs diagram can now be written as

$$\begin{aligned} \mathcal{M}_{Higgs} &= \left[-\frac{ig}{2\sqrt{2}M_W} V_{ub} \cot\beta m_b (1-\gamma_5)\right]\left[-\frac{i}{M_{H^\pm}^2}\right] \\ &\times \left[\frac{ig}{2\sqrt{2}M_W} \tan\beta m_\tau (1-\gamma_5)\right]\left[\frac{f_{B^+} m_{B^+}^2}{(m_u - m_b)}\right] \end{aligned} \tag{2.61}$$

where the first, second, and third square brackets contain the $H^+\bar{b}u$, H^+propagator (neglecting the momentum-squared relative to $M_{H^\pm}^2$), and $H^+\tau^+\nu_\tau$ Feynman rules respectively. The fourth square brackets contain the contribution to the matrix element from $\langle 0|\bar{b}\gamma_5 u|B^+\rangle$. Condensing and squaring terms in Eq. 2.61 the $\tan\beta$ dependence cancels giving

$$|\bar{\mathcal{M}}|^2_{Higgs} = \frac{g^4}{8M_W^4}|V_{ub}| f_{B^+}^2 m_\tau^2 (k'\cdot q')\left[\frac{m_{B^+}^4}{M_{H^+}^4}\right] \tag{2.62}$$

$$= |\bar{\mathcal{M}}|^2_{SM}\left[\frac{m_{B^+}^4}{M_{H^+}^4}\right]. \tag{2.63}$$

To calculate the interference diagram, we use the matrix elements from the Higgs and W^+ exchange diagrams and insert them into the expression for $2Re\mathcal{M}_{SM}\mathcal{M}^*_{Higgs}$

giving

$$
\begin{aligned}
2Re\mathcal{M}_{SM}\mathcal{M}^{*}_{Higgs} &= -2\left[\frac{g^4}{64M_W^4} f_{B^+}^2 m_\tau^2 |V_{ub}|^2 (q'\cdot k') \left(\frac{m_{B^+}}{M_{H^+}}\right)^2\right] \\
&= -2|\bar{\mathcal{M}}|^2_{SM}\left[\frac{m_{B^+}^2}{M_{H^+}^2}\right]. \qquad (2.64)
\end{aligned}
$$

Combining results and integrating over phase space the total width is

$$
\Gamma(B^+ \rightarrow \tau^+\nu_\tau) = \left[1-\frac{m_{B^+}^2}{M_{H^\pm}^2}\right]^2 \Gamma_{\rm SM}(B^+\rightarrow\tau^+\nu_\tau), \qquad (2.65)
$$

where the contributions from $W^+$and H^+ interfere destructively. In contrast, in the 2HDM-II, the total width including Higgs exchange is [43]

$$
\Gamma_{2HDM-II} = \left[1-\tan^2\beta\frac{m_{B^+}^2}{M_{H^\pm}^2}\right]^2 \Gamma_{SM}(B^+\rightarrow\tau^+\nu_\tau), \qquad (2.66)
$$

which using experimental results gives a contraint on the ratio $\frac{\tan\beta}{M_{H^\pm}}$ [53]. In the 2HDM-L there is no $\tan^2\beta$ factor due to the cancellation between the Yukawa couplings of the quarks, $y_q \propto \cot\beta$, and leptons, $y_\ell \propto \tan\beta$. Without the $\tan^2\beta$ enhancement, the new contribution from the charged Higgs exchange is very small as we can see from the calculation to follow.

The allowed charged Higgs mass values for the 2HDM-L can be found by re-arranging Eq. 2.65 and writing

$$
\left[1-\frac{m_{B^+}^2}{M_{H^\pm}^2}\right]^2 = \frac{8\pi\ {\rm BR}(B^+\rightarrow\tau^+\nu)}{\tau_{B^+} f_{B^+}^2 G_F^2 m_{B^+} m_\tau^2 |V_{ub}|^2 (1-m_\tau^2/m_{B^+}^2)^2}, \qquad (2.67)
$$

where τ_{B^+} is the B^+ lifetime. All quantities in Eq. 2.67 have been measured experimentally except for f_{B^+}, which can be taken from recent unquenched lattice QCD

results [44]:

$$f_{B^+} = f_B = 0.216 \pm 0.022 \text{ GeV}. \tag{2.68}$$

The current average experimental value of the branching ratio $B^+ \to \tau^+\nu_\tau$ comes from the BELLE and BABAR collaborations and is [45]:

$$BR(B^+ \to \tau^+\nu_\tau) = \left(1.41^{+0.43}_{-0.42}\right) \times 10^{-4}. \tag{2.69}$$

The only other quantity in Eq. 2.67 with a non-negligible uncertainty is $|V_{ub}|$, for which we take the global SM fit value [1],

$$|V_{ub}| = (3.59 \pm 0.16) \times 10^{-3}. \tag{2.70}$$

Combining all uncertainties in quadrature we obtain

$$\left[1 - \frac{m^2_{B^+}}{M^2_{H^\pm}}\right]^2 = 1.33 \pm 0.50, \tag{2.71}$$

which yields two allowed ranges for the charged Higgs mass at 95% CL:

$$0.63\, m_{B^+} \leq M_{H^\pm} \leq 0.80\, m_{B^+} \qquad \text{or} \qquad M_{H^\pm} \geq 1.5\, m_{B^+} = 8.1 \text{ GeV}. \tag{2.72}$$

Both of these mass ranges are too small to compete with the constraint found by the OPAL collaboration, Eq. 2.39.

2.2.43. $D_s^+ \to l^+\nu$

The leptonic decay $D_s^+ \to l^+\nu$ also proceeds in the Standard Model via the exchange

of a W^+ boson. This process is analogous to $B^+ \to \tau^+\nu_\tau$ and its partial width is given by

$$\Gamma\left(D_s^+ \to l^+\nu\right) = \frac{G_f^2}{8\pi} m_{D_s} f_{D_s}^2 m_l^2 |V_{cs}|^2 \left[1 - \frac{m_l^2}{m_{D_s}^2}\right]^2, \tag{2.73}$$

where m_{D_s} is the mass of the D_s meson and $|V_{cs}|$ is the applicable CKM matrix element. The D_s decay constant $f_{D_s}(p^2)$ is a function of the mass of the D_s meson and therefore a constant which is defined as

$$i f_{D_s} p_\mu = \langle 0 \left|\bar{s}\gamma_\mu\gamma_5 c\right| D_s(p)\rangle .$$

Recent improvements of the experimental and theoretical values of f_{D_s} have found up to a 3.8σ discrepancy between the two [46]. By assuming that only W bosons mediate $D_s^+ \to l^+\nu$, experimental results were used to obtain a value for the decay constant. Comparing the experimental central value $f_{D_s}^{expt} = 277 \pm 9$ MeV [46], with that of the most accurate lattice QCD calculation $f_{D_s}^{SM} = 241 \pm 3$ MeV [47], we find a 40% deviation from the expected Standard Model value. This deviation is given by

$$\frac{Expt.}{SM} = \left(\frac{f_{D_s}^{expt}}{f_{D_s}^{SM}}\right)^2 \simeq 1.40. \tag{2.74}$$

In the 2HDM-L, the partial width is

$$\Gamma(D_s^+ \to l^+\nu) = \left[1 - \frac{m_{D_s^+}^2}{M_{H^\pm}^2}\right]^2 \Gamma_{\rm SM}(D_s^+ \to l^+\nu), \tag{2.75}$$

which upon proceeding as we did in $B^+ \to l^+\nu$ and re-arranging Eq. 2.75 in terms of

$\left[1-\frac{m_{D_s^+}^2}{M_{H^\pm}^2}\right]^2$ gives

$$\left[1-\frac{m_{D_s^+}^2}{M_{H^\pm}^2}\right]^2 = \frac{8\pi\ \mathrm{BR}(D_s^+ \to l^+\nu)}{\tau_{D_s^+} f_{D_s^+}^2 G_F^2 m_{D_s^+} m_\tau^2 |V_{cs}|^2 (1-m_l^2/m_{D_s^+}^2)^2}. \tag{2.76}$$

The current experimental value of the $D_s^+ \to \tau^+\nu$ branching fraction is [1]

$$\mathrm{BR}(D_s^+ \to \tau^+\nu) = (6.6 \pm 0.6)\%. \tag{2.77}$$

Combining all uncertainties in quadrature as in the previous section and using the lattice QCD prediction for f_{D_s} we obtain

$$\left[1-\frac{m_{D_s^+}^2}{M_{H^\pm}^2}\right]^2 = 1.37 \pm 0.13 \tag{2.78}$$

which gives a more precise value than the previous approximation of Eq. 2.74. There is approximately a 40% difference between the SM value and experimental measurement. The destructive interference of the charged Higgs and W boson diagrams means that in order to account for this discrepancy, the charged Higgs mass at the 95% C.L. would have to be

$$M_{H^\pm} = (0.68 \pm 0.01) m_{D_s^+} = 1.34 \pm 0.02\ \mathrm{GeV} \tag{2.79}$$

which is excluded by direct searches. Thus we conclude that the discrepancy cannot be caused by the $H^\pm$ exchange in the 2HDM-L. Assuming the experimental central value and SM prediction were consistent, the 95% C.L. the allowed mass ranges from

Eq. 2.78 x

$$0.69\, m_{D_s^+} \leq M_{H^\pm} \leq 0.73\, m_{D_s^+}, \qquad M_{H^\pm} \geq 3.2\, m_{D_s^+} = 6.2 \text{ GeV}, \tag{2.80}$$

which are not only ruled out by OPAL but are also weaker than the constraint from $B^+ \to \tau^+\nu$.

2.2.44. Other Low Energy Processes

Other constraining processes studied in the literature for 2HDM's are $b \to c\tau\nu$ [48], $B^0_{(s)} \to ll$ [49], and $b \to s\gamma$ [50]. In the 2HDM-L, the first two processes do not give a constraint since the correction from H^+ is too small without the $\tan^2\beta$ enhancement found in other models, and the last process only involves the quark coupling and is simply constrained in the same way as the 2HDM-I.

The decay $b \to c\tau\nu$ proceeds in the 2HDM-L through virtual charged Higgs as well as $W^\pm$ bosons. Analogous to the process $B^+ \to \tau^+\nu$, the $\cot\beta$ dependence of the quark Yukawa coupling to $H^\pm$is cancelled by the $\tan\beta$ dependence of the coupling of charged Higgs to leptons. As well, there is a further suppression in $b \to c\tau\nu$ from integration over phase space since it is a $1 \to 3$ process.

In the Type-II 2HDM, the decay $B^0_{(s)} \to ll$ is enhanced by $\tan^2\beta$ from the charged Higgs couplings to down-type quarks and leptons. In the lepton-specific model, however, couplings of both up- and down-type quarks to the charged Higgs are proportional to $\cot\beta$ so once again the $\tan\beta$ and $\cot\beta$ dependence of the couplings cancel. This means the constraints from this process are weak compared to the LEP direct search.

As stated above, the loop-induced process $b \to s\gamma$ constrains the 2HDM-L in the

same way as it does the 2HDM-I since both models share the same Yukawa structure of charged Higgs couplings to quarks. In both models, this process is suppressed by a factor of $\cot^2\beta$ which comes from two couplings of $H^\pm$ to quarks. For this reason, parameter space can only be constrained for small values of $\tan\beta$. A lower bound of $\tan\beta \gtrsim 4$ (2) is found for $M_{H^\pm} = 100$ GeV (500 GeV) [25] but this observable provides no constraints for $\tan\beta > 4$.

2.2.5 Tevatron Direct Search

The Tevatron Collaborations CDF [51] and DØ [52] did a direct search for light charged Higgs bosons with $M_{H^\pm} < m_t - m_b$. The charged Higgs bosons are produced through the process $t \to bH^+$ and then decay via $H^+ \to c\bar{s}$ or $H^+ \to \tau\nu$. For $H^\pm \to c\bar{s}$, the invariant mass of the parent particle can be re-constructed from the quark jets and compared to the W boson mass. For the lepton specific model the partial width of the decay $t \to bH^+$ is proportional to $\cot^2\beta$ so the data from the Tevatron Collaborations only applies for $\tan\beta \sim 1$. In the region of parameter space $\tan\beta \simeq 2$ in Fig 2. of Ref. [53] there is a $\tan\beta$ dependent lower bound on the charged Higgs mass which ranges from the LEP bound to 160 GeV. This area of parameter space is already excluded by the $b \to s\gamma$ constraint which places a lower bound of $\tan\beta > 2$.

2.3 H^+ Branching Fractions

We now study the decay branching fractions of H^+ in the 2HDM-L calculated using `HDECAY` [54]. `HDECAY` is public `FORTRAN` code used to calculate charged Higgs decay

branching fractions for varying input parameters in the Minimal Supersymmetric Standard Model (MSSM). Adapting the coupling of charged Higgs to fermions in HDECAY by swapping the appropriate $\tan\beta$ and $\cot\beta$ in accordance with Eqs. 2.35 and 2.36, the branching ratios of $H^{\pm}$ as a function of $M_{H^{\pm}}$ were calculated for the 2HDM-L. Decays to $\phi^0 W^{\pm}$ (where $\phi^0 = A^0,\ h^0,\ H^0$) are included, however these decays depend on the scalar sector of the model and are equivalent to those of the Type-II model for equivalent parameter choices. For the decays to $h^0 W^{\pm}$ and $A^0 W^{\pm}$ we use M_{h^0} , M_{A^0}, and the $h^0 - H^0$ mixing angle as calculated using the MSSM mass relations in HDECAY with all supersymmetric mass parameters set to 1 TeV. Figures 2.4, 2.5, 2.6 and 2.7 show the branching ratios of $H^{\pm}$ as a function of $M_{H^{\pm}}$ for $\tan\beta = 5,\ 10,\ 20,$ and 100, respectively in the lepton-specific 2HDM. For comparison, equivalent plots are given for the Type-II 2HDM.

One can see that the Type-II and lepton-specific models behave similarly when $\tan\beta = 5$, except the decays to quarks are supressed in the lepton-specific model because the Yukawa couplings of both the up- and down-type quarks are proportional to $\cot\beta$. Decays to tb are still dominant above 180 GeV because the $m_t \cot\beta$ dependence of the $H^+ \to tb$ partial width is still much larger than the $m_\tau \tan\beta$ dependence of the $H^+ \to \tau^+\nu$ partial width. In Fig. 2.5, with $\tan\beta = 10$, $H^{\pm} \to \tau\nu$ dominates until the mass of the charged Higgs reaches 250 GeV where $H^{\pm} \to tb$ becomes the main decay mode. When $\tan\beta = 20$ decays to $H^{\pm} \to \tau\nu$ are completely dominant, and even above the top threshold decays to tb are less than 10%. Finally for $\tan\beta = 100$ and higher, the charged Higgs decays purely to leptons.

From Fig. 2.8 we see the total width of $H^{\pm}$ is composed of all the decay modes, but the predominant contributors are $H^{\pm} \to tb$ and $H^{\pm} \to \tau\nu$. When comparing the total widths of H^+ in the 2HDM-L and 2HDM-II, the behaviour of the graph reflects

the dependence of the bottom Yukawa coupling on $\tan\beta$. In both models below the top threshold, where the main decay is to $\tau\nu$, the behaviour of the total widths are similar. At 180 GeV the $\tan\beta$ dependence of each model becomes evident. Focusing on the total width plot of the lepton-specific model we can see that as $\tan\beta$ increases the severity of the change in the total width at the top threshold becomes minimal. This reflects the dominance of the charged Higgs decay to leptons, specifically $\tau\nu$. In the 2HDM-II, there is a severe change in the total width at the top threshold for all values of $\tan\beta$. This is because for charged Higgs masses greater than 180 GeV the dominant decay is $H^+ \to tb$ independent of $\tan\beta$.

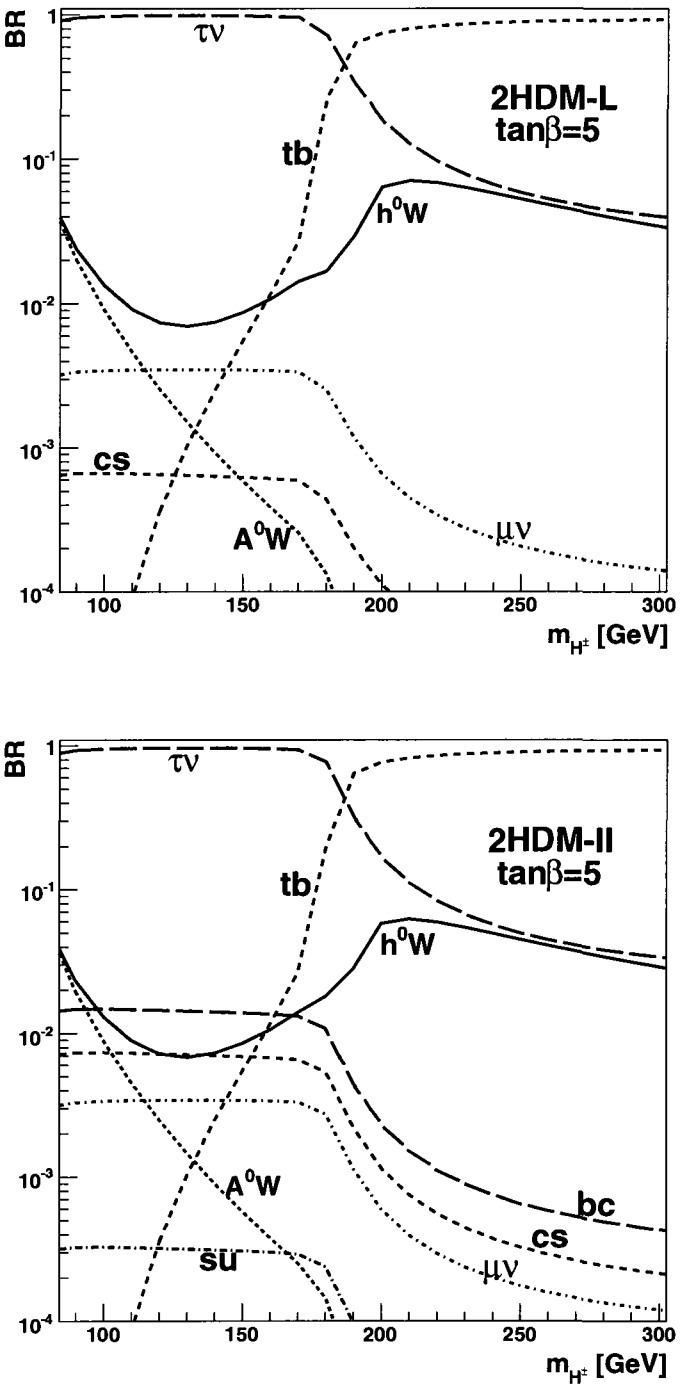

Figure 2.4: Branching ratios of $H^{\pm}$ as a function of $M_{H^{\pm}}$ for $\tan\beta = 5$.

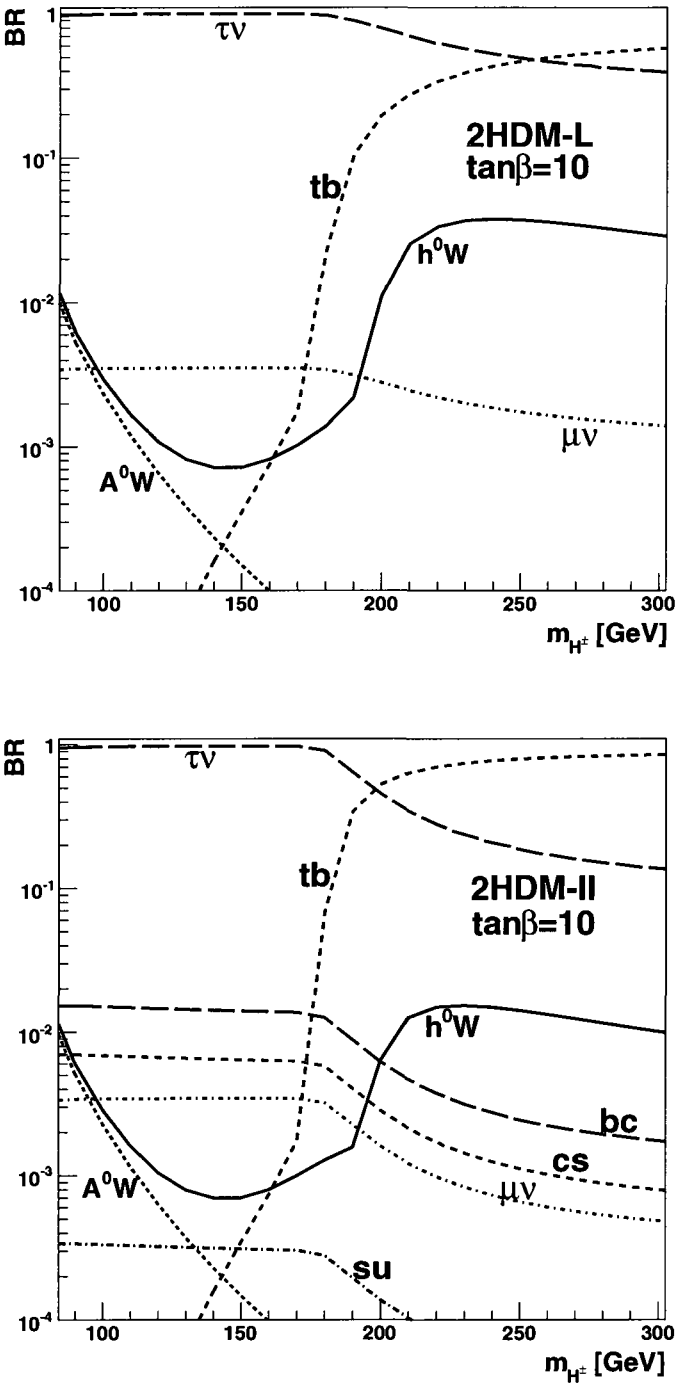

Figure 2.5: Branching ratios of $H^{\pm}$ as a function of $M_{H^{\pm}}$ for $\tan\beta = 10$.

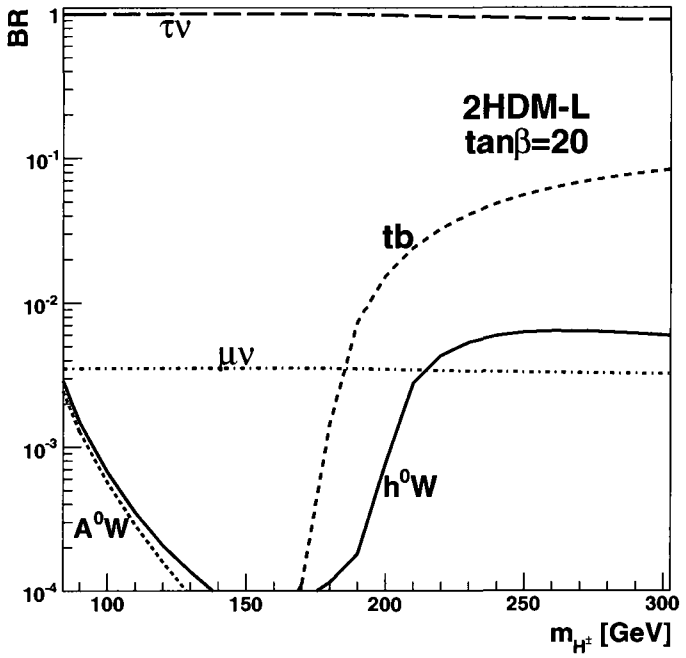

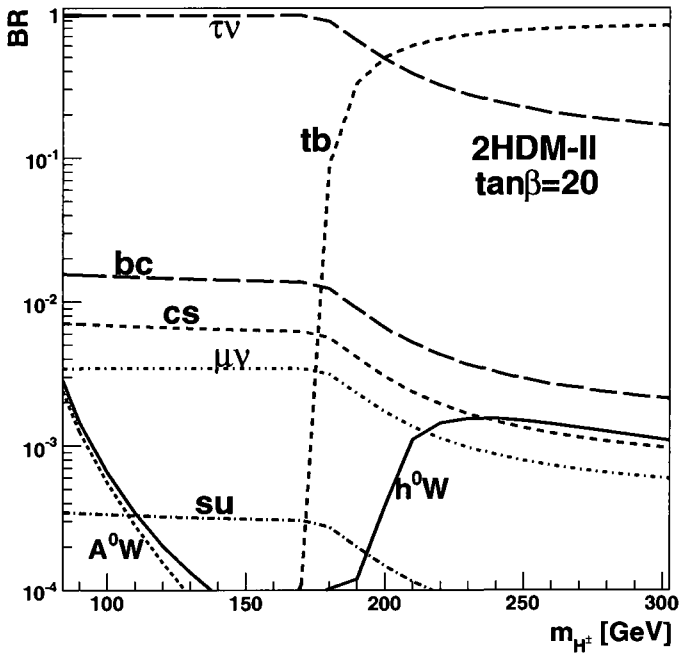

Figure 2.6: Branching ratios of $H^{\pm}$ as a function of $M_{H^{\pm}}$ for $\tan\beta = 20$.

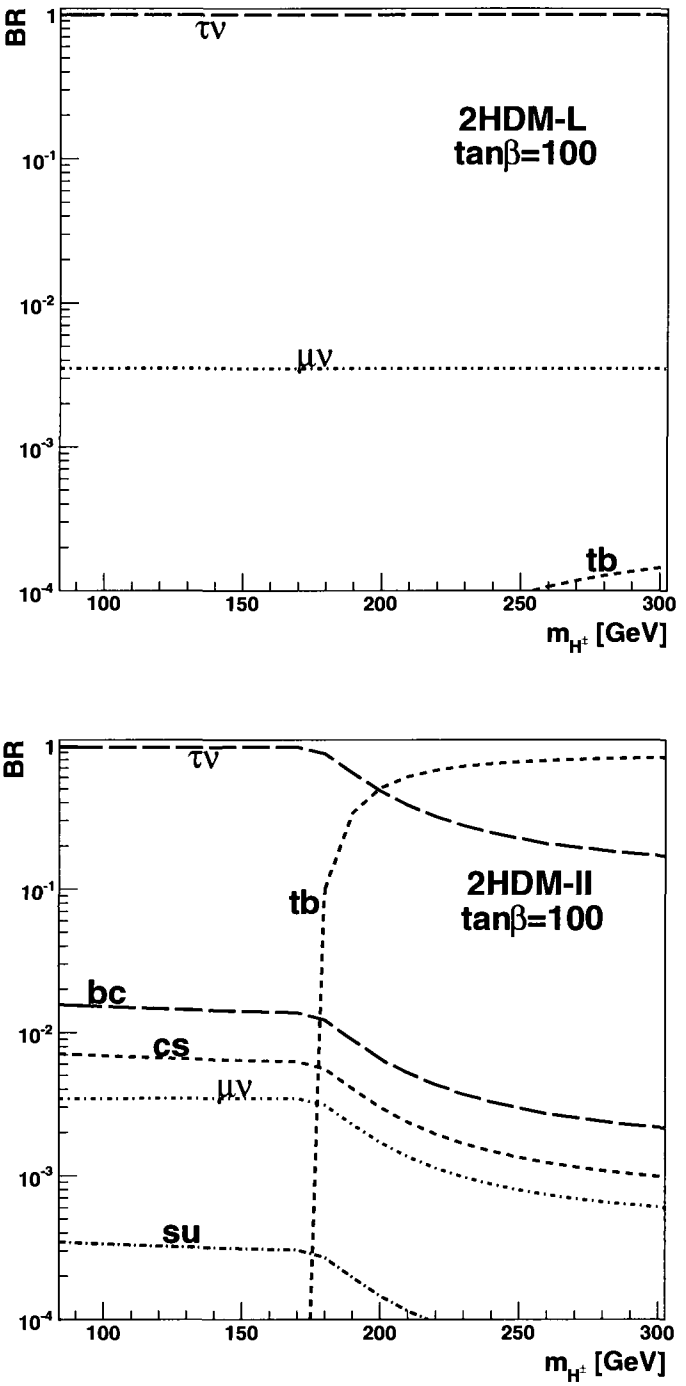

Figure 2.7: Branching ratios of $H^{\pm}$ as a function of $M_{H^{\pm}}$ for $\tan\beta = 100$.

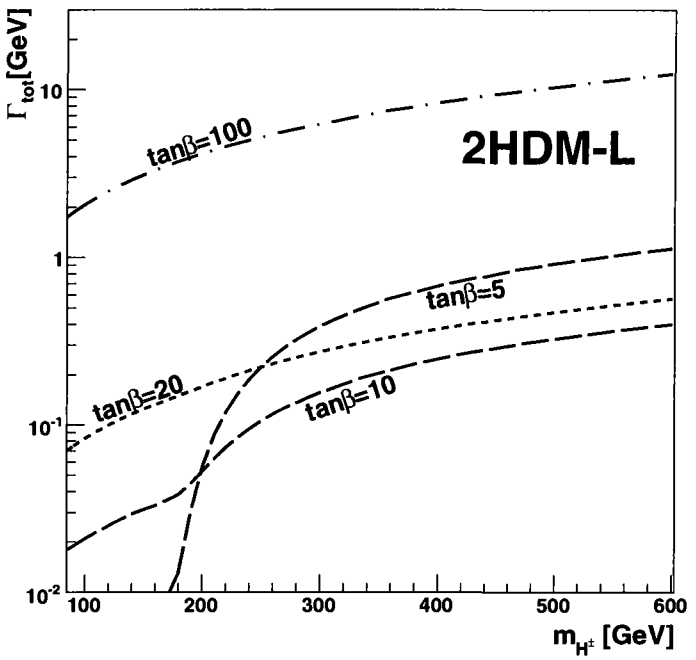

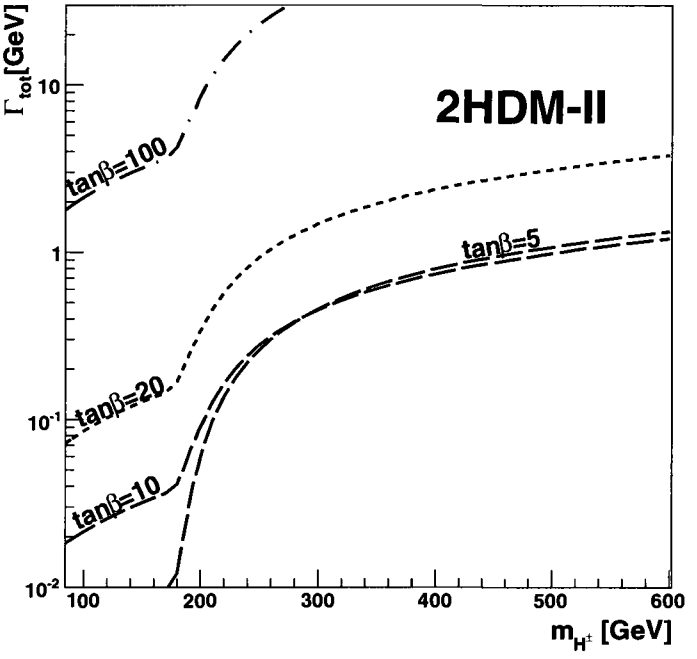

Figure 2.8: Total width of $H^{\pm}$ as a function of $M_{H^{\pm}}$ for varying $\tan\beta$=5, 10, 20, and 100.

2.4 LHC Search Prospects

The charged Higgs boson search channels that have been studied for the LHC have been those which would be best suited to a discovery in the Type-II 2HDM (MSSM). For the 2HDM-II, it is expected that charged Higgs bosons will be produced in association with either top quarks or W bosons, and will decay mainly to $b\bar{t}$, $\tau\bar{\nu}$, and Wh^0. Studies by ATLAS [55] and CMS [56] have concluded that the most promising channel is $pp \to tH^-$ with the charged Higgs decaying to $\tau\nu$ or tb [40]. In the 2HDM-II, this particular process is enhanced by a factor of $\tan^2\beta$ which boosts the production cross section at large $\tan\beta$. In the 2HDM-L however, the Yukawa coupling of the quarks have both terms proportional to $\cot\beta$ (see Eq. 2.35) and this production process is actually supressed by $\cot^2\beta$. Here we survey prospects in the 2HDM-L.

2.4.1 Light Charged Higgs

For masses $M_{H^\pm} < m_t - m_b$ the main production mode that has been studied by ATLAS and CMS is $q\bar{q} \to t\bar{t} \to \bar{t}bH^+$ where one top quark decays via $t \to bH^+$ and the other decays via $t \to Wb$. For this mass range in the Type-II model, which these studies have been based upon, the charged Higgs is expected to decay via $H^+ \to \tau\nu$ for all values of $\tan\beta \gtrsim 1$. Referencing figures 2.4, 2.5, 2.6, and 2.7, one can see that in the lepton specific model $H^+ \to \tau\nu$ is the dominant decay mode for all $\tan\beta$ values and charged Higgs masses less than 180 GeV. Therefore, the analysis for the Type-II model can be applied directly . We apply the 5σ charged Higgs discovery sensitivity quoted in Ref. [57] to the lepton-specific model by computing the tree level branching ratio of $t \to H^+b$ and translating it into a lower bound on $\tan\beta$ as a function of $M_{H^\pm}$.

The branching ratio at tree level is

$$BR(t \to H^+ b) = \frac{\Gamma_{H^+}}{\Gamma_W + \Gamma_{H^+}} \tag{2.81}$$

and the calculated partial widths neglecting m_b are given by

$$\Gamma_{H^+} = \frac{G_F}{8\sqrt{2}\pi} m_t^3 \cot^2\beta \left[1 - \frac{M_{H^+}^2}{m_t^2}\right]^2 \quad \text{and} \quad \Gamma_W = \frac{G_F}{8\sqrt{2}\pi} m_t^3 \left(1 + \frac{2m_W^2}{m_t^2}\right) \left[1 - \frac{m_W^2}{m_t^2}\right]^2 . \tag{2.82}$$

Inserting the branching ratio reach for $t \to H^+ b$ found by ATLAS we find the LHC discovery reach with 30 fb^{-1} to be $\tan\beta \lesssim 4.9$ (4.6, 2.4) for $M_{H^\pm} = 100$ (120, 150) GeV.

2.4.2 Heavy Charged Higgs

The main charged Higgs production processes studied by ATLAS and CMS are those which take advantage of the $\tan\beta$-enhanced bottom Yukawa coupling in the 2HDM-II. In the lepton-specific model, all bottom-induced processes will instead be supressed by powers of $\cot\beta$. Some of these processes are charged Higgs pair production through $b\bar{b} \to H^+H^-$ and $gg \to H^+H^-$, as well as $W^\pm H^\mp$ associated production. The first two processes are suppressed since their cross sections are proportional to $\cot^4\beta$ and the third process is suppressed by $\cot^2\beta$. This dependence along with the loop suppression factor for the gluon fusion and small parton density of the bottom quarks makes it impossible to observe these processes in our model.

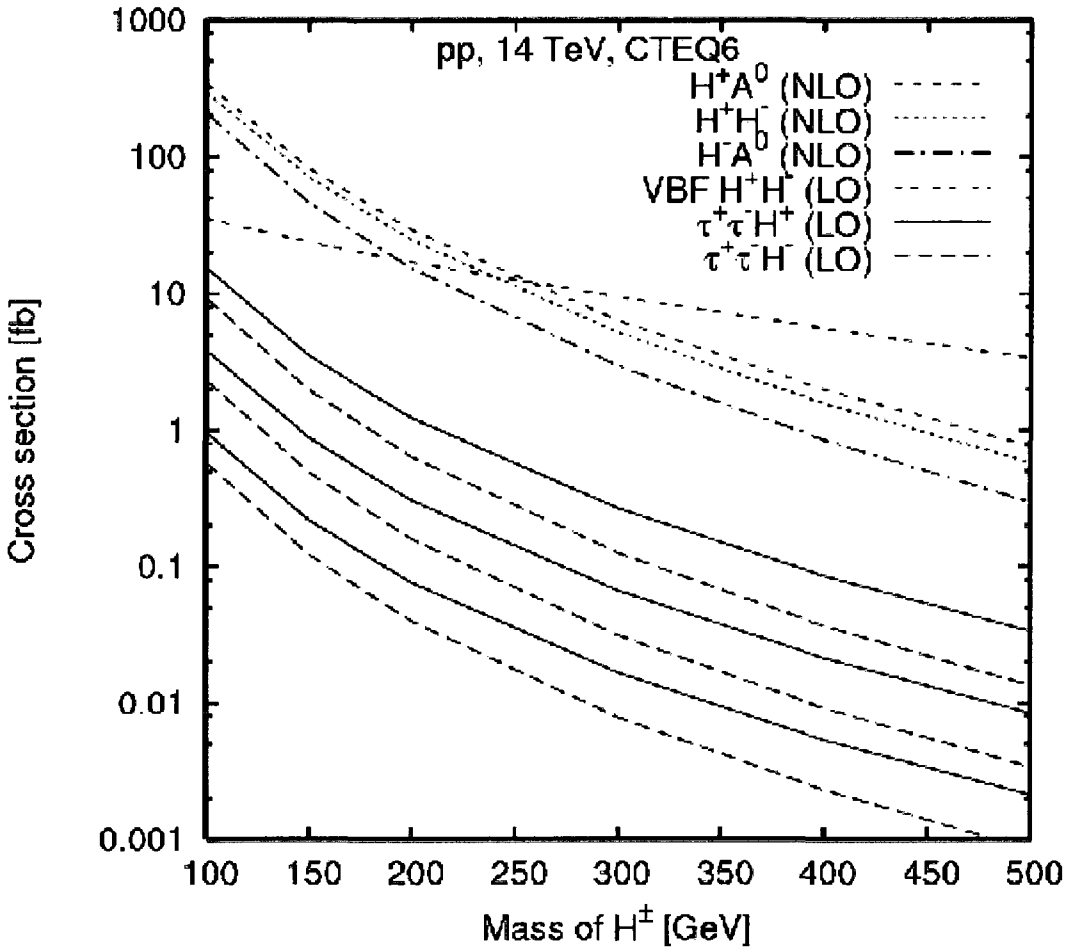

Figure 2.9: Cross sections for charged Higgs production at the LHC. The solid (dashed) lines show the cross sections for $\tau^+\tau^- H^+$ ($\tau^+\tau^- H^-$) production via Yukawa radiation for $\tan\beta = 200$, 100, and 50 from top to bottom. [From Ref. [29]]

Figure 2.9 (from Ref. [29]) shows cross sections for charged Higgs production in the lepton-specific model at the LHC. Pair production of charged Higgs bosons can proceed through an s-channel Z or photon, or through vector boson fusion (VBF) $qq \to qqV^*V^* \to qqH^+H^-$ ($V = \gamma,\ Z,\ W^\pm$). These processes depend only on electroweak couplings and are therefore not unique to the lepton-specific model. From Fig. 2.9 one can see that the s-channel process is larger than VBF for $M_{H^\pm} \lesssim 250$ GeV;

for masses above 250 GeV, the VBF cross section is dominant. The dominant search channel in this model will be $pp \rightarrow H^+H^- \rightarrow \tau\nu\tau\nu$. Pair produced charged Higgs have a large cross section and the decays to leptons should provide a clean signature.

Associated production of $H^{\pm}$with a CP-odd (CP-even) neutral Higgs boson is also not specific to the lepton-specific model; these cross sections are dependent only on the relevant scalar masses (scalar masses and CP-even mixing angle α). If the CP-even mixing angle is chosen such that the $W^+H^-h^0$ coupling vanishes, then the $H^{\pm}H^0$ cross section is equal to the $H^{\pm}A^0$ cross section for $M_{H^0} = M_{A^0}$.

It is also possible to radiate a charged Higgs off of a final state tau lepton. The squared matrix element for $\bar{q}q' \rightarrow W^{+*} \rightarrow \tau^+\tau^-H^+$is given by

$$\sum_{spins} |\mathcal{M}|^2 = g^4 \left[\frac{gm_\tau}{\sqrt{2}M_W} \tan\beta\right]^2 \frac{4p_2 \cdot k_1[2(k_2 \cdot k_3)(p_1 \cdot k_3) - M^2_{H^\pm}(p_1 \cdot k_2)]}{(q^2 - M_W^2)^2[2(k_1 \cdot k_3) + M^2_{H^\pm}]^2} \tag{2.83}$$

where p_1, p_2, k_1, k_2, and k_3 are the four-momenta of the incoming $\bar{q}$ and q', and outgoing τ^+, τ^-, and H^+. Eq. 2.83 shows the dependence of the cross section on $\tan\beta$, and from Fig. 2.9 it is clear that even enhancement from large $\tan\beta$ values does not allow this process to compete with $pp \rightarrow H^+H^- \rightarrow \tau\nu\tau\nu$.

Chapter 3

The Flipped 2HDM

3.1 The Model

The name of this model comes from the Yukawa structure as compared to the 2HDM-II. If one modifies the Yukawa structure of the 2HDM-II by coupling the leptons to the same doublet as the up-type quarks then one recovers the flipped 2HDM where the lepton couplings have 'flipped' from one doublet to the other. Once again we have two complex SU(2) Higgs doublets

$$\Phi_u = \begin{pmatrix} \phi_u^+ \\ \frac{1}{\sqrt{2}}\left(\phi_u^{0,r} + v_u + i\phi_u^{0,i}\right) \end{pmatrix}, \qquad \Phi_d = \begin{pmatrix} \phi_d^+ \\ \frac{1}{\sqrt{2}}\left(\phi_d^{0,r} + v_d + i\phi_d^{0,i}\right) \end{pmatrix}. \tag{3.1}$$

The kinetic Lagrangian and scalar potential in the flipped 2HDM are identical to those in Eqs. 2.4 and 2.5 with $\Phi_q \to \Phi_u$, $\Phi_\ell \to \Phi_d$, and the Yukawa Lagrangian is

given by

$$\mathcal{L}_{Yukawa} = \sum_i \sum_j \left[y^u_{ij} \overline{u}_{Ri} \widetilde{\Phi}^\dagger_u Q_{Lj} + y^d_{ij} \overline{d}_{Ri} \Phi^\dagger_d Q_{Lj} + y^e_{ij} \overline{e}_{Ri} \Phi^\dagger_u L_{Lj} \right] + h.c. \tag{3.2}$$

where the correct structure is enforced by imposing a $\mathbb{Z}_2$ symmetry

$$\Phi_d \to -\Phi_d, \qquad d_{Rj} \to -d_{Rj} \tag{3.3}$$

with all other fields invariant. Defining conventions we have the free parameter

$$\tan\beta \equiv \frac{v_u}{v_d}, \tag{3.4}$$

and the charged Higgs boson is a linear combination of fields from the two complex SU(2) Higgs doublets

$$H^\pm = -\sin\beta \phi^\pm_d + \cos\beta \phi^\pm_u. \tag{3.5}$$

In the quark mass basis the Yukawa Lagrangian for the charged Higgs in this model is

$$\mathcal{L}_{flipped} = \sum_{i,j=1}^{3} \frac{g}{\sqrt{2} M_W} H^+ \left[V_{ij} m_{ui} \cot\beta \bar{u}_i P_L d_j + V_{ij} m_{dj} \tan\beta \bar{u}_i P_R d_j + m_{\ell i} \cot\beta \bar{\nu}_i P_R \ell_i \right] + h.c. \tag{3.6}$$

and the charged Higgs couplings can be read off as

$$H^+ \bar{u}_i d_j \;\; : \;\; \frac{ig}{\sqrt{2} M_W} V_{ij} (\cot\beta m_{ui} P_L + \tan\beta m_{dj} P_R) \tag{3.7}$$

$$H^+ \bar{\nu} \ell \;\; : \;\; \frac{ig}{\sqrt{2} M_W} \cot\beta m_\ell P_R. \tag{3.8}$$

One can see from the above equations that the $H^+\bar{u}_L d_R$ term contributes a coupling proportional to $m_d \tan\beta$, the $H^+\bar{u}_R d_L$ term gives a coupling proportional to $m_u \cot\beta$, and the lepton couplings are proportional to $m_\ell \cot\beta$.

3.1.1 Perturbativity of y_t and y_b

The allowed range of $\tan\beta$ for this model can be determined from the perturbativity of the top and bottom quark Yukawa couplings. In Sec. 2.1.4, perturbativity of the tau Yukawa coupling was used to set an upper bound on $\tan\beta$ in the lepton-specific model. Once again, the Yukawa couplings must be less than or equal to 4π in order to make perturbation theory a valid approximation. Starting with

$$y_t = \frac{\sqrt{2}m_t}{v_{SM}\ \sin\beta} \qquad \text{and} \qquad y_b = \frac{\sqrt{2}m_b}{v_{SM}\ \cos\beta} \tag{3.9}$$

we can make the approximations

$$y_t \simeq \frac{\sqrt{2}m_t \cot\beta}{v_{SM}} \qquad \text{and} \qquad y_b \simeq \frac{\sqrt{2}m_b \tan\beta}{v_{SM}} \tag{3.10}$$

for $\tan\beta \ll 1$ and $\tan\beta \gg 1$ respectively.

Substituting $m_t = 171.3$ GeV [1], $m_b = 4.20$ GeV ($\overline{MS}$ mass [1]) and $v_{SM} = 246$ GeV, the allowed $\tan\beta$ range for $y_{t,b} \leq 2$ is

$$0.49 \ \leq \tan\beta \leq 82.8 \tag{3.11}$$

and the allowed $\tan\beta$ range for $y_{t,b} \leq 1$ is

$$0.98 \leq \tan\beta \leq 41.4. \tag{3.12}$$

3.2 Experimental Constraints

The experimental constraints on the flipped model will be identical to those on the 2HDM-II for processes involving only quarks. Those processes involving leptons will be suppressed compared to the 2HDM-II at large $\tan\beta$ and therefore the constraints will be much weaker. First we give a summary of the latest results of constraints on $M_{H^\pm}$ from $b \to s\gamma$ in the 2HDM-II and flipped 2HDM and then discuss processes which give less stringent constraints. $b \to s\gamma$ places a lower limit on the charged Higgs mass $M_{H^\pm} \gtrsim 295$ GeV, and an existing experimental constraint from LEP-II gives a $BR(H^+ \to \tau^+\nu)$ independent lower bound $M_{H^\pm} > 78.0$ GeV at the 95% C.L.

3.2.1 $b \to s\gamma$

The process $b \to s\gamma$ proceeds in the SM through one-loop diagram(s) mediated by a W boson and top quark. In any 2HDM there is also a charged Higgs contribution in addition to the Standard Model W boson. The constraints on the charged Higgs mass and $\tan\beta$ in the Type-II model have been studied extensively in the literature [48,58,59,60,61,62] and due to the identical quark Yukawa structure of the flipped and Type-II models the constraints on these parameters will be identical in both models.

In order to incorporate QCD corrections this process is treated using an effective theory in which the loop is approximated by a single vertex that couples the bottom

quark, strange quark and photon. The effective Hamiltonian density is found by integrating out the heavy particles ($W^{\pm}$, t, $H^{\pm}$) and parametrizing the effects of these particles using an operator product expansion. This effective Hamiltonian is given by [58]

$$\mathcal{H}_{eff} = \frac{4G_F}{\sqrt{2}} V_{ts}^* V_{tb} \sum_{j=1}^{8} C_j(\mu) \mathcal{O}_j(\mu) \tag{3.13}$$

where V_{ts} and V_{tb} are CKM matrix elements and the effective operators with explicit color indices are [58]

$$\begin{aligned}
\mathcal{O}_1 &= (\bar{c}_{L\beta}\gamma^{\mu} b_{L\alpha})(\bar{s}_{L\alpha}\gamma_{\mu} c_{L\beta}), \\
\mathcal{O}_2 &= (\bar{c}_{L\alpha}\gamma^{\mu} b_{L\alpha})(\bar{s}_{L\beta}\gamma_{\mu} c_{L\beta}), \\
\mathcal{O}_3 &= (\bar{s}_{L\alpha}\gamma^{\mu} b_{L\alpha}) \left[(\bar{u}_{L\beta}\gamma_{\mu} u_{L\beta}) + ... + (\bar{b}_{L\beta}\gamma_{\mu} b_{L\beta})\right], \\
\mathcal{O}_4 &= (\bar{s}_{L\alpha}\gamma^{\mu} b_{L\beta}) \left[(\bar{u}_{L\beta}\gamma_{\mu} u_{L\alpha}) + ... + (\bar{b}_{L\beta}\gamma_{\mu} b_{L\alpha})\right], \\
\mathcal{O}_5 &= (\bar{s}_{L\alpha}\gamma^{\mu} b_{L\alpha}) \left[(\bar{u}_{R\beta}\gamma_{\mu} u_{R\beta}) + ... + (\bar{b}_{R\beta}\gamma_{\mu} b_{R\beta})\right], \\
\mathcal{O}_6 &= (\bar{s}_{L\alpha}\gamma^{\mu} b_{L\beta}) \left[(\bar{u}_{R\beta}\gamma_{\mu} u_{R\alpha}) + ... + (\bar{b}_{R\beta}\gamma_{\mu} b_{R\alpha})\right], \\
\mathcal{O}_7 &= \left(e/16\pi^2\right) m_b \bar{s}_{L\alpha}\sigma^{\mu\nu} b_{R\alpha} F_{\mu\nu}, \\
\mathcal{O}_8 &= \left(g_s/16\pi^2\right) m_b \bar{s}_{L\alpha}\sigma^{\mu\nu} T^a_{\alpha\beta} b_{R\beta} G^a_{\mu\nu}.
\end{aligned}$$

Here L, R are the helicities of the u, s, c, b quarks, α, β are colour indices, $F_{\mu\nu}$ ($G^a_{\mu\nu}$) are the field strength tensors of the electromagnetic (strong) forces, m_b is the bottom quark mass, $T^a_{\alpha\beta}$ are the $SU(3)_C$ generators and μ is an energy scale which is discussed in more detail after Eq. 3.21.

In order to determine the effective coefficients it is necessary to calculate the loop diagrams of the full Lagrangian to be able to match the coefficients $C_j(\mu)$ of the operator

product expansion in Eq. 3.13. Evaluating the full Lagrangian using perturbation theory and comparing the results to Eq. 3.13 the leading order SM coefficients that contribute to $b \to s\gamma$ are [58]

$$\begin{aligned} C_2(M_W) &= 1, && (3.14)\\ C_j(M_W) &= 0, \quad j = 1,3,4,5,6 && (3.15)\\ C_7(M_W) &= -\frac{1}{2}A(x), && (3.16)\\ C_8(M_W) &= -\frac{1}{2}D(x), && (3.17) \end{aligned}$$

with $x = m_t^2/M_W^2$ and

$$\begin{aligned} A(x) &= x\left[\frac{\frac{2}{3}x^2 + \frac{5}{12}x - \frac{7}{12}}{(x-1)^3} - \frac{(\frac{3}{2}x^2 - x)\ln\ x}{(x-1)^4}\right],\\ D(x) &= \frac{x}{2}\left(\frac{\frac{1}{2}x^2 - \frac{5}{2}x - 1}{(x-1)^3} + \frac{3x\ \ln\ x}{(x-1)^4}\right). \end{aligned} \tag{3.18}$$

Including the extended Higgs sector of the flipped 2HDM the SM coefficents $C_7(M_W)$ and $C_8(M_W)$ are modified as follows [58]

$$\begin{aligned} C_7(M_W) &= -\frac{1}{2}A(x) - B(y) - \frac{1}{6}\cot^2\beta\ A(y), && (3.19)\\ C_8(M_W) &= -\frac{1}{2}D(x) - \frac{1}{6}\cot^2\beta\ D(y) - E(y), && (3.20) \end{aligned}$$

where $y = \frac{m_t^2}{M_{H^\pm}^2}$, $A(x)$ and $D(x)$ are defined above and

$$B(y) = \frac{y}{2}\left(\frac{\frac{5}{6}y - \frac{1}{2}}{(y-1)^2} - \frac{(y - \frac{2}{3})}{(y-1)^3}\ \ln\ y\right), \qquad E(y) = \frac{y}{2}\left[\frac{\frac{1}{2}y - \frac{3}{2}}{(y-1)^2} + \frac{\ln\ y}{(y-1)^3}\right]. \tag{3.21}$$

In order to have a full description of the effective theory, it is necessary to scale down the dependence of the coefficients from the high energy regime to those energies valid for the bottom quark mass. This is done through the anomalous dimension matrix which accounts for the renormalization of operators including mixing. The relationship between the coefficients $C_j(M_W)$ and $C_j(M_b)$, where M_b denotes the bottom quark pole mass, are found by explicitly solving the renormalization group equations [58]

$$\mu\frac{d}{d\mu}C_j(\mu) - \sum_{j=1}^{8}\gamma_{ij}(g_s)C_i(\mu) = 0 \tag{3.22}$$

to find the matrix equation

$$C(M_b) = \left[\exp\int_{g_s(M_W)}^{g_s(M_b)} dg\frac{\gamma^T(g_s)}{\beta(g_s)}\right] C(M_W), \tag{3.23}$$

where g_s is the strong gauge coupling and γ_{ij} is the anomalous dimension matrix (see Ref. [58]). The branching ratio at leading logarithmic order is given by [48]

$$BR(\bar{B} \to X_s\gamma) = \frac{|V_{ts}^*V_{tb}|^2}{|V_{cb}|^2}\frac{6\alpha_{em}}{\pi g(x)}|C_7(M_b)|^2 BR(\bar{B} \to X_c e\bar{\nu}_e) \tag{3.24}$$

where $\alpha_{em} = e^2/4\pi$ is the electromagnetic fine structure constant, $C_7(M_b)$ is given by Eq. 3.23, and $g(x) = 1 - 8x^2 + 8x^6 - x^8 - 24x^4\ln x$ is a phase space factor with $x = M_c/M_b$ (ratio of the charm and bottom quark pole masses).

This process has been studied extensively for the Type-II 2HDM up to next to leading order (NLO) [61] and more recently at next-to-next-to-leading order (NNLO) [48, 59, 62] for the SM part. The lower bound on the charged Higgs mass is extremely sensitive to the experimental central value and uncertainty of the branching ratio as well as the theoretical prediction for the SM. Various studies have found SM values of branching

ratios for $b \to s\gamma$ ranging from $(2.98 \pm 0.26) \times 10^{-4}$ (Ref. [59]) to $(3.15 \pm 0.23) \times 10^{-4}$ (Ref. [62]) which correspond to lower bounds on the charged Higgs mass between about 200-300 GeV. Following the work of Misiak et al. [62] We take the SM NNLO branching ratio

$$\mathcal{B}(\bar{B} \to X_s\gamma) = (3.15 \pm 0.23) \times 10^{-4} \tag{3.25}$$

and current experimental value [45]

$$\mathcal{B}(\bar{B} \to X_s\gamma) = (3.55 \pm 0.24^{+0.09}_{-0.10} \pm 0.03) \times 10^{-4} \tag{3.26}$$

which at the 95% C.L. gives a lower bound on the charged Higgs mass

$$M_{H^\pm} \geq 295 \text{ GeV} \tag{3.27}$$

which is constant for $\tan\beta$ values of 2 or greater. For values of $\tan\beta$ greater than 2, the $\cot\beta$ terms in Eqs. 3.19 and 3.20 are too small to contribute; for values less than 2 these terms do contribute. At $\tan\beta \leq 2$, the relationship can no longer be approximated as linear and the behaviour for these values can be seen in the curve labelled $B \to X_s\gamma$ in Fig. 3.1 taken from Fig. 2 of Ref. [48].

The asymptotic lower bound on the charged Higgs mass from Fig. 3.1 differs from that of Eq. 3.27 due to the use of different experimental central values and the χ^2 values used for Fig. 3.1 do not translate exactly to the 95% C.L. used in Eq. 3.27.

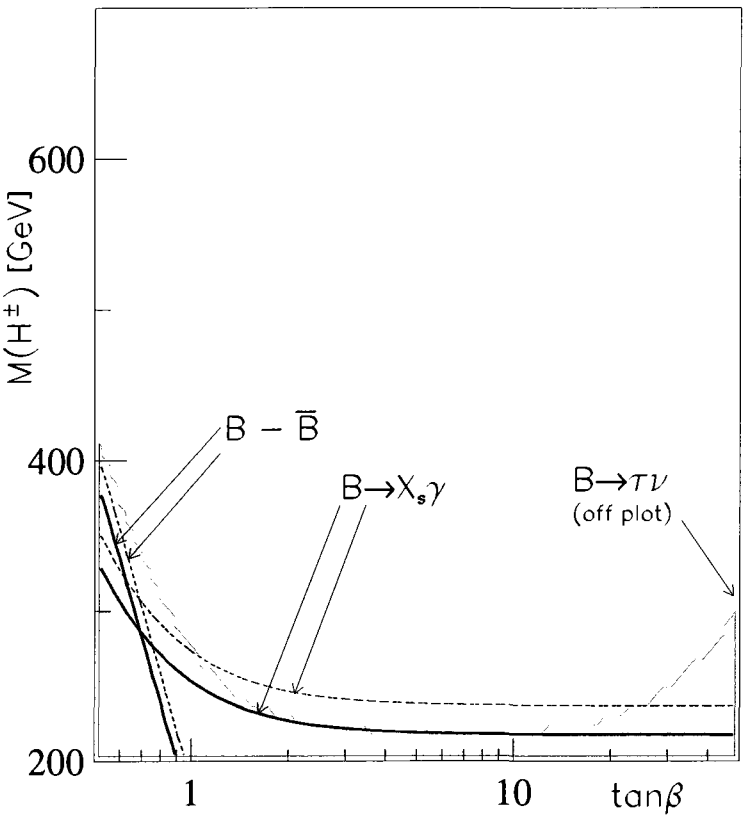

Figure 3.1: Small $\tan\beta$ behaviour of the lower bound on $M_{H^\pm}$from $b \to s\gamma$ at the 90% C.L. (dashed) and 95% C.L. (solid). Graph taken from Fig. 2 of Ref. [48].

3.2.2 LEP-II Direct Constraint

In 2001 the four LEP collaborations combined their results to place a lower bound on $M_{H^\pm}$ which varied with the allowed decay modes of $H^\pm$ [31]. In each case charged Higgs bosons are pair produced and for the combined result they are assumed to decay into either $\tau\nu$ or $c\bar{s}$. In the flipped 2HDM this assumption is invalid as the dominant hadronic decay for all values of $\tan\beta > 1$ and $M_{H^\pm} \leq 180$ GeV is bc, as will be seen in Figs. 3.3, 3.4, 3.5 of Sec. 3.3.

The individual collaborations ALEPH [63] and OPAL [30] placed a limit on the charged Higgs mass as a function of $BR(H^+ \to \tau^+\nu)$ which is not sensitive to the quark flavor and is only constrained by the assumption $BR(H^+ \to \tau^+\nu) + BR(H^+ \to q\bar{q}) = 1$. L3 [64] and DELPHI [65] also placed limits on the charged Higgs mass, except they used techniques such as explicit charm tagging or a b veto to only include those events where $H^+ \to cs$; as such, these studies can not be applied to the Flipped 2HDM . OPAL and ALEPH considered the events $q\bar{q}q\bar{q}$, $q\bar{q}\tau\nu$, $\tau^+\nu\tau^-\bar{\nu}$ and OPAL also considered final states involving the CP-odd Higgs boson A^0 which is used to constrain the 2HDM-I. To place a lower bound on the charged Higgs mass for the Flipped 2HDM we take the the more stringent lower bound from the ALEPH collaboration. The $BR(H^+ \to \tau^+\nu)$ independent lower bound at the 95% C.L is [63]

$$M_{H^+} > 78.0 \text{ GeV} \tag{3.28}$$

but for $BR(H^+ \to \tau^+\nu) = 0$ (1) it can increase to

$$M_{H^\pm} \geq 80.7 \text{ (83.4) GeV}. \tag{3.29}$$

This constraint is well below the limit set by $b \to s\gamma$; however, it has been set by a direct search and is not subject to change from new physics beyond the SM.

3.2.3 Tevatron Direct Search

The Tevatron Collaborations CDF [51] and DØ [52] did a direct search for light charged Higgs bosons with $M_{H^\pm} < m_t - m_b$ in the context of the Type-II 2HDM. The charged Higgs bosons are produced through $pp \to t\bar{t}$ with one top quark decaying

via $t \to W^{\pm}b$ and the other top quark decaying via $t \to bH^{+}$; $H^{\pm}$ are then assumed to decay to $c\bar{s}$ or $\tau\nu$. For the lepton specific model the partial width of the decay $t \to H^{+}b$ is proportional to $\cot^2\beta$ so the data from the Tevatron Collaborations only applies for $\tan\beta \sim 1$. In the Flipped model however, the partial width of the decay $t \to H^{+}b$ is given by

$$\Gamma(t \to H^{+}b) = \frac{G_F}{8\sqrt{2}\pi}\left[m_t^3 \cot\beta + m_t m_b^2 \tan\beta\right]\left[1 - \frac{M_{H^{\pm}}^2}{m_t^2}\right]^2, \qquad (3.30)$$

so the data from CDF and DØ applies for both high and low $\tan\beta$. Reference [51] presented the 95 % CL upper limit on $BR(t \to H^{+}b)$ with $H^{+} \to cs$ as a function of $M_{H^{\pm}}$. Applying this limit to the flipped 2HDM by computing the tree-level branching ratio of $t \to H^{+}b$, upper bounds were placed on $\tan\beta$. At high $\tan\beta$ the charged Higgs decays dominantly to bc in the Flipped 2HDM whereas the data from CDF and DØ has been based on the Type-II model where the charged Higgs decays to cs. The only difference in the reconstruction of the charged Higgs should be in the energy resolution of the $H^{\pm}$ mass peak due to missing energy from the bottom quark decaying weakly. We note that this will affect the limits as they apply to this model, but should not significantly change the results. To find lower bounds on $\tan\beta$ we are able to apply the DØ analysis for the Type-II model directly [52]. The branching ratios of the charged Higgs decays are nearly identical in both the Flipped and Type-II models for $\tan\beta \sim 1$ so the lower bounds on $\tan\beta$ can be read directly from Fig. 11 of Ref. [52]. The following bounds were placed on $\tan\beta$,

$$\text{For } M_{H^{\pm}} = 100 \text{ GeV}, \quad 1.40 \leq \tan\beta \leq 28.8, \qquad (3.31)$$

$$\text{For } M_{H^{\pm}} = 120 \text{ GeV}, \quad 1.10 \leq \tan\beta \leq 26.2, \qquad (3.32)$$

$$\text{For } M_{H^{\pm}} = 150 \text{ GeV}, \quad 0.53 \leq \tan\beta \leq 65.8. \qquad (3.33)$$

In Eqs. 3.31, 3.32, and 3.33, the lower bound on $\tan\beta$ becomes weaker for increasing $M_{H^\pm}$. If only considering accessible phase space in the $t \to H^+b$ decay, one would expect the same type of behaviour for the upper bound. The unexpected upper bound on $\tan\beta$ for $M_{H^\pm} = 100$ GeV comes from the weaker limit on $BR(t \to H^\pm b)$ due to a larger background as $M_{H^\pm}$ approaches $M_{W^\pm}$. For $M_{H^\pm} = 120$ GeV, the limit on the BR is stronger and the upper bound on $\tan\beta$ bceomes more restrictive. As $M_{H^\pm}$ increases to 150 GeV, the lack of phase space dominates and the upper bound on $\tan\beta$ becomes weaker as expected. Perturbativity of the top and bottom Yukawa couplings with $y_{t,b} \leq 2$ gives the range of allowed values $0.49 \leq \tan\beta \leq 82.8$. Comparing this range with Eqs. 3.31, 3.32, and 3.33, one can see that parameter space at both low and high $\tan\beta$ is excluded by the $t \to H^+b$ constraint. We note however that these charged Higgs masses are already disfavoured by $b \to s\gamma$.

3.2.4 Other Low Energy Constraints

Unlike the leptonic 2HDM, the flipped 2HDM is not able to utilize lepton universality in τ decay, or the Michel parameters in μ or τ decay, to obtain contraints on the ratio of the charged Higgs mass and $\tan\beta$ since the leptonic Yukawa coupling of the 2HDM-F is proportional to $\cot\beta$. This structure will also not be constrained by processes such as $B^+ \to \tau^+\nu$, $D^+ \to \tau^+\nu$, $b \to c\tau\nu$, $B^0_{(s)} \to \ell^+\ell^-$ since in each of these cases the $\cot\beta$ dependence of the lepton coupling will either cancel with the $\tan\beta$ dependence of the down-type quark coupling or combine with the $\cot\beta$ dependence of the up-type quark coupling to suppress the H^+contribution to the cross section by $\cot^2\beta$.

3.3 Branching Fractions

The branching fractions of the charged Higgs in the flipped 2HDM are presented in Figs. 3.2, 3.3, 3.4, and 3.5 for $\tan\beta = 1,\ 5,\ 10,$ and 50 respectively. These branching ratios were again computed using a modified version of the public FORTRAN code `HDECAY`, which in its original form computes SM Higgs and Minimal Supersymmetric Model (MSSM) Higgs decays. To adapt `HDECAY` for the flipped 2HDM, the couplings involved in the decay of charged Higgs bosons were modified according to Eqs. 3.7 and 3.8 and decays to supersymmetric particles were not included. For ease of comparison the branching fractions for the same parameters in the 2HDM-II are included.

For $\tan\beta = 1$ (Fig. 3.2) one can see that the branching fractions of the 2HDM-II and 2HDM-F are identical. This is because the couplings of quarks are identical in both models, and when $\tan\beta = \cot\beta = 1$, the couplings to leptons are also the same. At $\tan\beta = 5$ (Fig. 3.3), decays to leptons are already severely suppressed as a result of the $\cot\beta$ dependence of the lepton Yukawa couplings. Due to the identical structure of the quark Yukawa couplings in the 2HDM-II and 2HDM-F, the hierarchy of quark branching fractions remains the same but to compensate for the suppression of decays to $\tau\nu$ the branching ratios to bc, cs, and su are strongly enhanced below 180 GeV where decays to top quarks are kinematically inaccessible. The limit $M_{H^\pm} \geq 295$ GeV set by $b \to s\gamma$ disfavours this region of parameter space and we expect the charged Higgs mass to fall above this bound.

As $\tan\beta$ gets larger the suppression of leptons increases. When $\tan\beta = 50$, the branching ratios to leptons are smaller than 10^{-4} and hadronic decays completely dominate.

In the Type-II 2HDM, the charged Higgs decays to cs at low $\tan\beta$ ($H^\pm cs \sim m_c \cot\beta$)

and to $\tau\nu$ at high $\tan\beta$ ($H^{\pm}\tau\nu \sim m_{\tau}\tan\beta$) . In the Flipped 2HDM, the charged Higgs decay to cs is proportional to $(m_c\cot\beta + m_s\tan\beta)V_{cs}$, the charged Higgs decay to cb is proportional to $(m_c\cot\beta + m_b\tan\beta)V_{cb}$, and the charged Higgs decay to $\tau\nu$ is proportional to $m_{\tau}\cot\beta$. $m_bV_{cb} > m_sV_{cs}$ so as $\tan\beta$ increases, the bottom Yukawa coupling dominates and the charged Higgs decays to cb.

The total width of the charged Higgs boson as a function of $M_{H^{\pm}}$ is shown in Fig. 3.6 for $\tan\beta$ values of 1, 5, 10, and 50 in both the flipped and Type-II 2HDM. As expected from the identical structures, the total width of the charged Higgs is identical in both models for $\tan\beta = 1$. For $M_{H^{\pm}} \leq 180$ GeV other values of $\tan\beta$ show the difference in the Yukawa structure of the two models. For values above the top threshold, both models are dominated by decays to tb which is evident from the similar behaviour in this region.

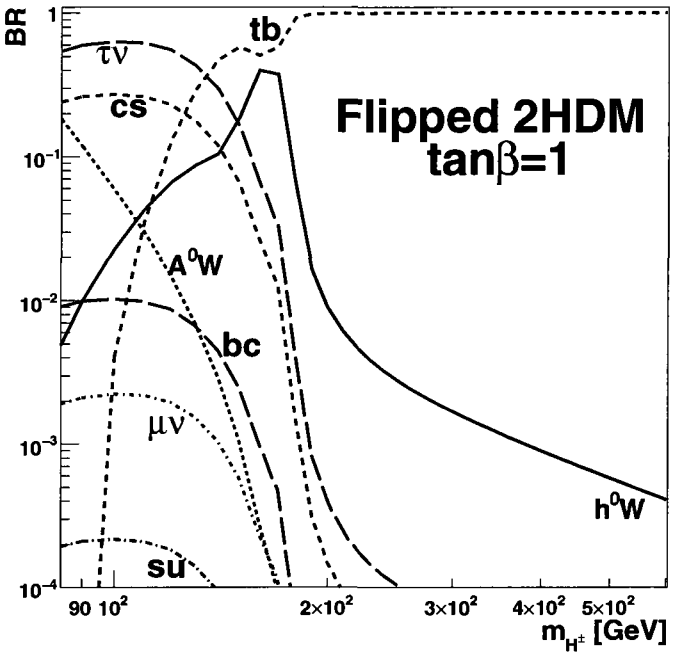

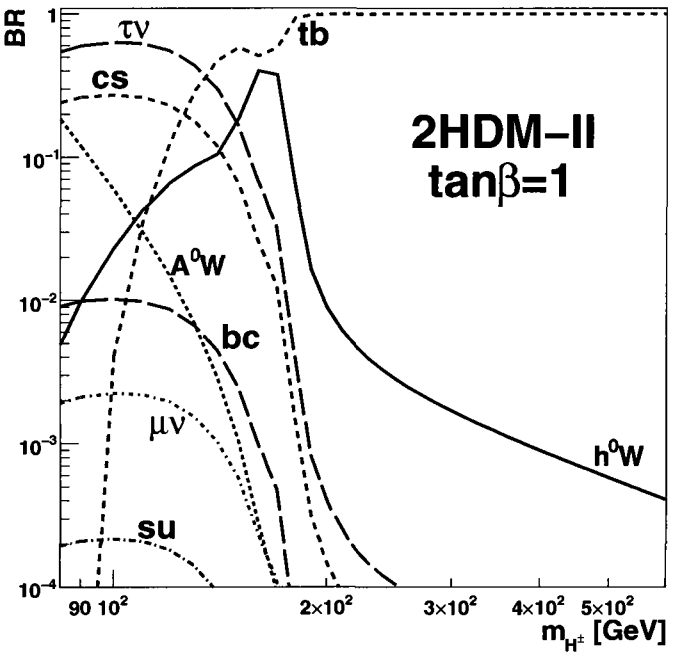

Figure 3.2: Branching ratios of $H^\pm$ as a function of $M_{H^\pm}$ for $\tan\beta = 1$.

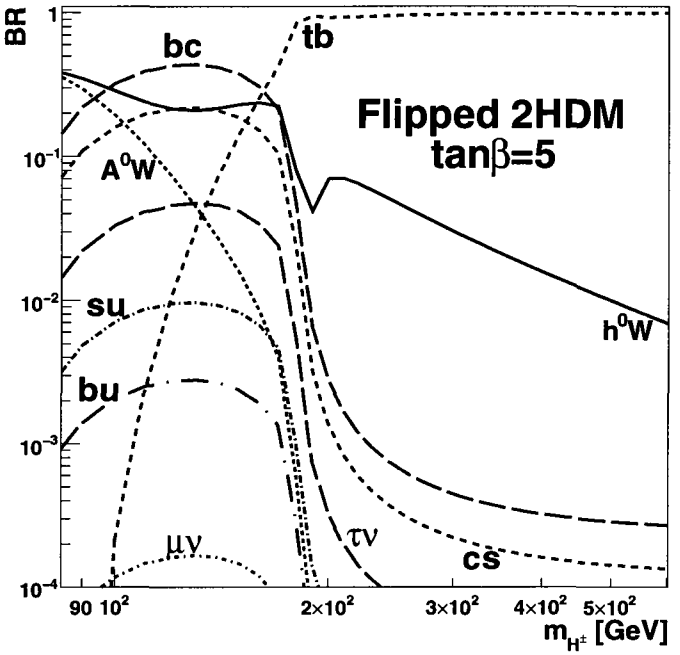

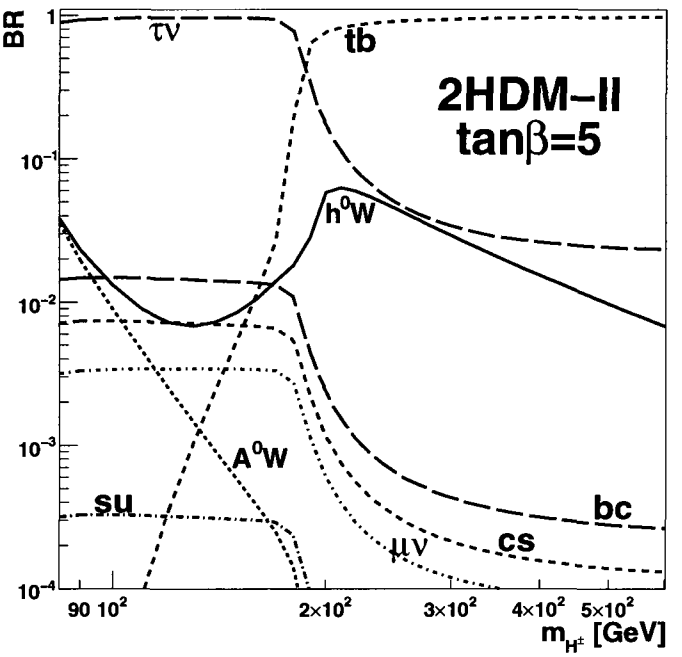

Figure 3.3: Branching ratios of $H^{\pm}$ as a function of $M_{H^{\pm}}$ for the flipped 2HDM with $\tan\beta = 5$.

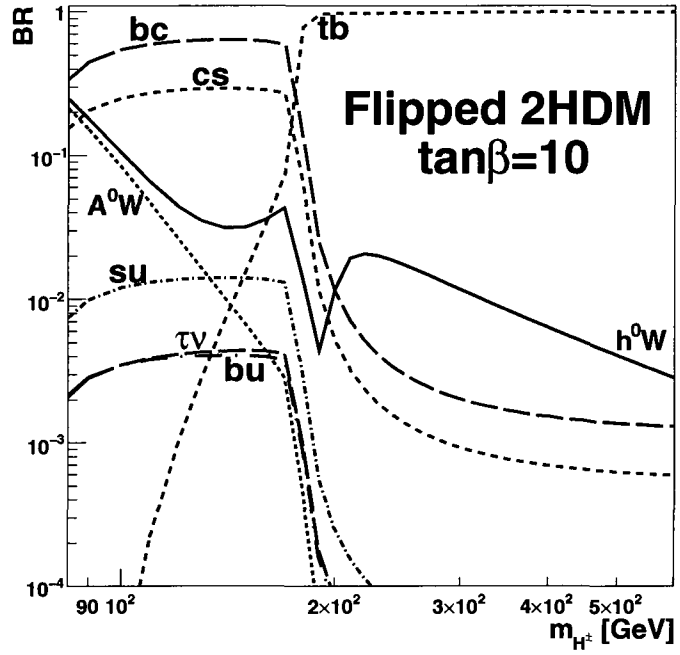

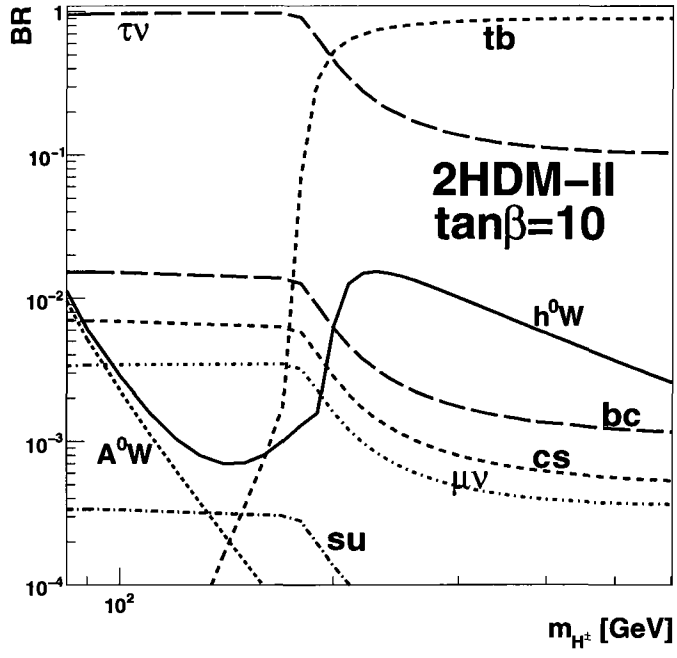

Figure 3.4: Branching ratios of $H^{\pm}$ as a function of $M_{H^{\pm}}$ for $\tan\beta = 10$.

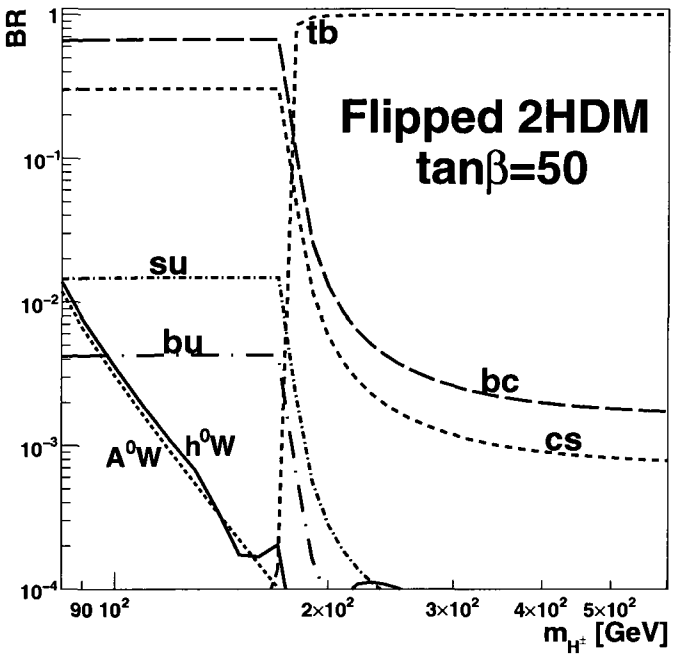

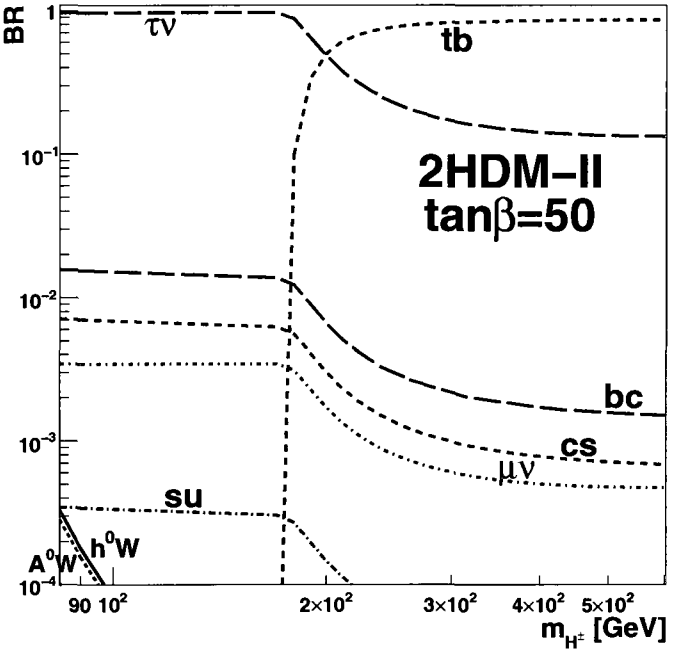

Figure 3.5: Branching ratios of $H^{\pm}$ as a function of $M_{H^{\pm}}$ for $\tan\beta = 50$.

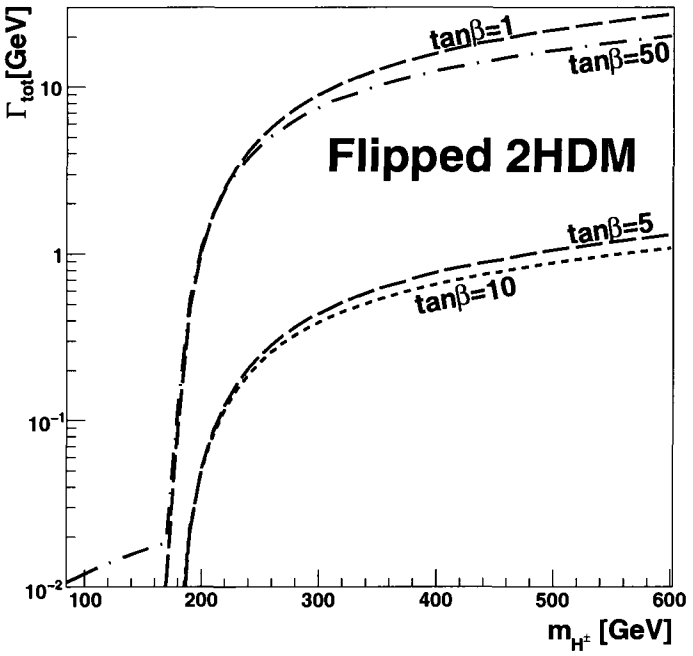

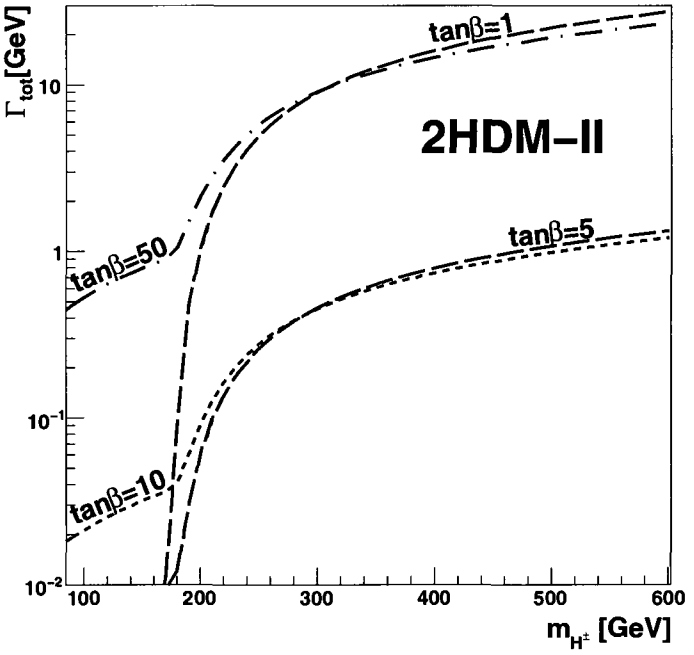

Figure 3.6: Total width of $H^{\pm}$ as a function of $M_{H^{\pm}}$ with varying $\tan\beta$ for the Flipped 2HDM and 2HDM-II.

3.4 LHC Search Prospects

The charged Higgs search channels that have been studied by ATLAS and CMS are those which utilize the Yukawa structure of the Type-II 2HDM. Since the Yukawa structure of the flipped 2HDM is identical to that of the 2HDM-II in the quark sector, many of the same LHC charged Higgs production channels apply. Due to the $\tan\beta$ dependence of the bottom Yukawa coupling, processes that take advantage of the coupling of the charged Higgs to the bottom quark have been studied in depth. In these models radiating a charged Higgs off of a bottom quark will give the biggest enhancement because the $H^{\pm}tb$ coupling will boost the production cross section by $\tan^2\beta$. The main difference of discovery processes in the Flipped 2HDM compared to the 2HDM-II comes from the suppression of charged Higgs decays to leptons. In the 2HDM-II, below the top threshold, the charged Higgs decays to $\tau\nu$ for all values of $\tan\beta$ above 1 due to the dependence of the tau Yukawa coupling on this parameter. In the Flipped 2HDM, the tau Yukawa coupling is proportional to $\cot\beta$ and this impacts the search prospects that have been studied for the Type-II model using $\tau\nu$ as a final state.

3.4.1 Light Charged Higgs

For masses $M_{H^{\pm}} < m_t - m_b$ the main production mode that has been studied is $q\bar{q} \rightarrow t\bar{t} \rightarrow \bar{t}bH^+$ where one top quark decays via $t \rightarrow bH^+$and the other via $t \rightarrow bW$. For this mass range in the Type-II model, which these studies have been based upon, the charged Higgs is expected to decay via $H^+ \rightarrow \tau\nu$ for all values of $\tan\beta \gtrsim 1$. Referencing figures 3.3, 3.4, and 3.5, one can see that in the flipped model $H^+ \rightarrow bc$ is the dominant decay mode for $\tan\beta$ values greater than 1 and charged Higgs masses

less than 180 GeV. Since the studies up until this point assume $H^+ \to \tau\nu$, no information can be extracted and applied to this model.

The best search channel in this model would be a top quark decaying to a light charged Higgs with the Higgs decaying via $H^\pm \to bc$. The Tevatron collaborations CDF and DØ have studied this channel and consider the possibility of the charged Higgs decaying purely to $\tau\nu$ or purely to cs [51,52]. These searches could be adapted by ATLAS and CMS to look for the charged Higgs decaying to bc which would account for all other values of $\tan\beta > 1$. A particularily useful search would be $t\bar{t} \to Wb\, H^+b$ where the W boson decays leptonically to provide a trigger and the charged Higgs decays to cb. The mass of the parent particle could be reconstructed from momentum of the charm and bottom quarks and compared to that of the W boson. Since the decay $W \to cb$ is suppressed from the CKM matrix, this could be a promising way to find a charged Higgs in this area of parameter space if b tagging is used.

3.4.2 Heavy Charged Higgs

For charged Higgs masses greater than the top quark mass the most frequently studied search channels are $H^\pm t$ associated production [66], H^+W^- associated production [67], and $b\bar{b} \to H^+H^-$ [40]. In each of these cases the matrix element will be enhanced by up to two factors of $\tan\beta$ arising from the $H^\pm tb$ couplings, which corresponds to cross sections enhanced by up to $\tan^4\beta$.

3.4.21. $H^\pm t$ Associated Production

The charged Higgs can be produced in association with a top quark through bottom-gluon fusion $gb \to tH^+$ and through gluon fusion $gg \to \bar{b}tH^-$. The inclusive and

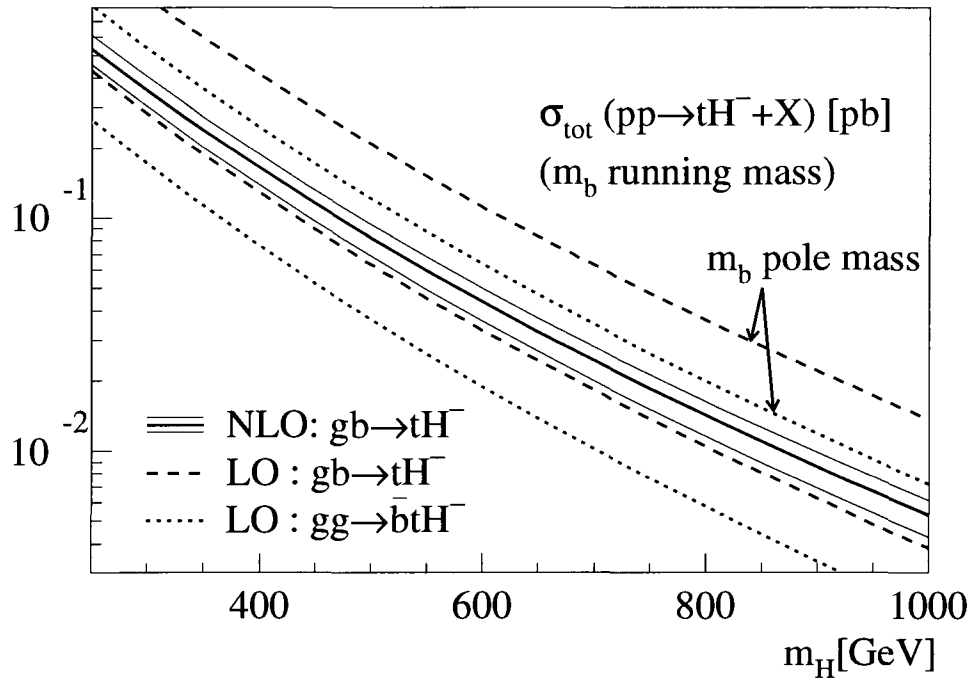

Figure 3.7: The LO and NLO cross section of $gb \to tH^-$ as a function of $M_{H^\pm}$ at the LHC with $\tan\beta = 30$ [From Ref [66]].

exclusive processes were studied in Ref. [66] and the most promising search channel for charged Higgs bosons in this model is the inclusive process $gb \to tH^+$. The leading order (LO) and next-to-leading order cross sections for bottom-gluon fusion are plotted as a function of $M_{H^\pm}$ in Fig. 4 of Ref. [66], reproduced in Fig. 3.7. In Fig. 3.7 the NLO cross section for a charged Higgs of mass $M_{H^\pm} = 200$ GeV can be read off as $\sigma_{tot}(gb \to tH^-) \sim 0.4$ pb $= 400$ fb for $\tan\beta = 30$.

In the Flipped model, for $\tan\beta > 1$ and $M_{H^\pm} > m_t - m_b$, the dominant decay of the charged Higgs is $H^\pm \to tb$ which is the same as in the Type-II 2HDM. The current studies by the LHC collaborations ATLAS and CMS are based on the 2HDM-II so in this region of parameter space the analysis can be applied directly. ATLAS and CMS [57] find an accessible charged Higgs mass region as a function of $\tan\beta$ using 30 fb^{-1} of data. For $\tan\beta = 30$ (45, 60), ATLAS and CMS expect a 5-sigma discovery

reach for $M_{H^\pm}$ between approximately 180 and 200 (250, 300) GeV in the $gb \to tH^+$, $H^+ \to tb$ search channel [57].

3.4.22. Pair Produced $H^\pm$

Charged Higgs bosons can be pair produced in the tree level Drell-Yan process $q\bar{q} \to H^+H^-$, loop induced gluon fusion $gg \to H^+H^-$, and bottom quark scattering $b\bar{b} \to H^+H^-$. Ref [40] made a detailed study of the cross sections of these processes and found that at low values of $\tan\beta$ the cross section is largest for the Drell-Yan process while at large values of $\tan\beta$ the loop induced process has the largest cross section. This is because the loop induced process is enhanced by two H^+tb couplings which means the cross section is proportional to $\tan^4\beta$. At large values of $\tan\beta$ this enhancement surpasses the loop supression and the loop-induced processes dominate. The following LHC cross sections are taken from [40] for $M_{H^\pm} = 200$ GeV and given as a function of $\tan\beta$,

$$\sigma(q\bar{q} \to H^+H^-) = 26 \text{ fb} \qquad \text{independent of } \tan\beta, \tag{3.34}$$

$$\sigma(gg \to H^+H^-) = 0.21\ (2,\ 10,\ 79) \text{ fb} \qquad \text{for } \tan\beta = 10\ (20,\ 30,\ 50), \tag{3.35}$$

$$\sigma(b\bar{b} \to H^+H^-) = 0.13\ (0.15,\ 0.57,\ 6.2) \text{ fb} \qquad \text{for } \tan\beta = 10\ (20,\ 30,\ 50). \tag{3.36}$$

The Drell-Yan process dominates with a $\tan\beta$ independent cross section of 26 fb which is only exceeded by loop-induced gluon fusion which takes over between $\tan\beta = 30$ and $\tan\beta = 50$. For $\tan\beta = 50$ gluon fusion has a cross section of $\sigma(gg \to H^+H^-) = 79$ fb .

For charged Higgs masses below 180 GeV and $\tan\beta \lesssim 5$, the charged Higgs will

decay to $\tau\nu$. In this same mass range for moderate values $\tan\beta \gtrsim 5$ the charged Higgs decays to bc, $H^+H^- \rightarrow b\bar{c}\bar{b}c$. Unless $H^\pm \rightarrow bc$ is found to be a viable search channel this process will be indistinguishable from background. Above 180 GeV for all values of $\tan\beta$ the charged Higgs decays to tb with top quarks decaying via $t \rightarrow Wb$, $H^+H^- \rightarrow t\bar{b}\bar{t}b \rightarrow b\bar{b}b\bar{b}W^+W^-$.

3.4.23. $H^\pm W$ Associated Production

Another possible search channel is producing a charged Higgs boson in association with a W boson. $W^\pm H^\mp$ associated production can proceed through $b\bar{b}$ annihilation at tree level or gluon fusion at one loop. The W boson is then expected to decay leptonically which could easily be detected. The cross sections for $b\bar{b}$ annihilation and gluon fusion are [67]

$$\sigma(b\bar{b} \rightarrow W^\pm H^\mp) = 190\ (24,\ 255)\ \text{fb} \qquad \text{for} \quad \tan\beta = 1.5\ (6,\ 30) \tag{3.37}$$

and

$$\sigma(gg \rightarrow W^\pm H^\mp) = 80\ (5,\ 4.6)\ \text{fb} \qquad \text{for} \quad \tan\beta = 1.5\ (6\ , 30) \tag{3.38}$$

with a charged Higgs mass of $M_{H^\pm} = 200$ GeV. From the values given we can see that the contribution to $W^\pm H^\mp$ associated production from $b\bar{b}$ annihilation is dominant for all values of $\tan\beta$. At small $\tan\beta \sim 1$ the cross section from $b\bar{b}$ anhillation is larger than that of gluon fusion by a little more than a factor of 2, however as $\tan\beta$ increases to 30 this factor increases to approximately 50. The cross section for moderate $\tan\beta$

values is smaller than for small or large values of $\tan\beta$. This is because at small $\tan\beta$, the top mass contribution to the coupling $H^{\pm}tb \sim (m_t \cot\beta + m_b \tan\beta)$ is still sizeable. As $\tan\beta$ increases, the top mass contribution becomes smaller which decreases the cross section. At large $\tan\beta$ the bottom mass term is enhanced and the cross section grows again.

In this mass range, the charged Higgs will decay to tb. The signal will be $W^{\pm}H^{\mp} \to \ell\nu tb$, where the lepton can be used for a trigger and the top quark decays via $t \to Wb$. At the LHC, $t\bar{t} \to W^+W^-b\bar{b}$ is bound to be a large background, however the invariant mass of $jjbb$ from $H^{\pm}$ decay reconstructs to $M_{H^{\pm}}$.

3.4.24. Electroweak Processes

In this model there is also vector boson fusion $qq \to qqVV \to qqH^+H^-$ where $V = \gamma,\ Z,\ W^{\pm}$, and charged Higgs pair production via an s-channel Z boson or photon. A full description of these processes was given for the lepton-specific 2HDM in Sec. 2.4. Since these are not model specific processes, Sec. 2.4 can be referenced for more information.

Chapter 4

Conclusions

Experimental confirmation of a charged Higgs boson would conclusively prove beyond the Standard Model physics and shed light on the process of electroweak symmetry breaking. The most theoretically promising model is the Type-II two Higgs doublet model which is compatible with supersymmetry and is the basis of all current experimental studies for the LHC. In this thesis I have focused on two other models, the Flipped and Lepton-specific 2HDM's, in which the charged Higgs mass can be constrained by applying existing experimental data.

4.1 General Features

The unique signatures of each model come from the Yukawa couplings of the charged Higgs to fermions. In the Type-II 2HDM, the coupling of down-type quarks and leptons (up-type quarks) to charged Higgs bosons are proportional to $\tan\beta$ ($\cot\beta$). In the 2HDM-L, the coupling of the charged Higgs to leptons (up- and down-type quarks) are proportional to $\tan\beta$ ($\cot\beta$). Finally, in the 2HDM-F couplings of the

charged Higgs to down-type quarks (up-type quarks, leptons) are proportional to $\tan\beta$ ($\cot\beta$) so processes involving only quarks will be identical in the 2HDM-II and 2HDM-F.

Imposing perturbative constraints on the Yukawa couplings of each model bounds the free parameter $\tan\beta$. In the lepton specific model an upper bound of $\tan\beta \lesssim 1200$ was calculated from requiring the tau Yukawa coupling $y_\tau < 4\pi$; more moderate values of the coupling were used giving the upper limits $\tan\beta \leq 100$ (200) corresponding to $y_\tau \leq 1$ (2). Focusing on larger values of $\tan\beta$ where $BR(H^+ \to \tau^+\nu) \simeq 1$ was useful in determining the lower bound on the charged Higgs mass from LEP-II. The Flipped 2HDM yielded allowed values 0.49 (0.97) $\leq \tan\beta \leq 84.2$ (42.1) for $y_{t,b} \leq 2$ (1).

4.2 Indirect Constraints

The strongest indirect constraint in the lepton-specific 2HDM came from lepton universality in tau decays. When the Higgs sector of the SM is extended to include two doublets (and hence charged Higgs bosons) then the tau leptons can decay via charged Higgs as well as $W^\pm$ bosons. Including the charged Higgs diagram and interference, taking the ratio of $\tau \to \mu\nu\nu$ and $\tau \to e\nu\nu$ and comparing to the exerimental value, two allowed mass ranges $0.61\tan\beta$ GeV $\leq M_{H^\pm} \leq 0.73\tan\beta$ GeV or $M_{H^\pm} \geq 1.4\tan\beta$ GeV were found at the 95% C.L. It was also shown that if the experimental value of g_μ/g_e is improved to better than 0.05%, as expected at SuperB, then the allowed mass ranges would become $0.64\tan\beta$ GeV $\leq M_{H^\pm} \leq 0.67\tan\beta$ GeV or $M_{H^\pm} \geq 3.2\tan\beta$ GeV. This process does not constrain the Flipped 2HDM since the charged Higgs contribution to the tau lepton decay amplitude is proportional to $\cot^2\beta$, which cannot be large.

In the lepton-specific model, the Michel parameters were a natural choice for constraints since they parametrize the phase space distribution of decaying tau leptons. This particular decay in the 2HDM-L is enhanced by a factor of $\tan\beta$, so a constraint on the ratio $\frac{M_{H^\pm}}{\tan\beta}$ could be found. The Michel parameters in the SM are constants and upon introducing charged Higgs exchange were modified by factors of $m_L m_\ell \frac{\tan\beta}{M_{H^\pm}}$. The decays of muons gave extremely weak constraints due to the small muon mass, whereas the decays of taus gave stronger constraints due to their heavier mass but were still too weak to compete with lepton universality since the Michel parameters were not measured to good enough precision.

The strongest indirect constraint in the Flipped 2HDM came from the process $b \to s\gamma$ which was identical to the constraint from this process in the Type-II 2HDM. In the SM this process proceeds through virtual $W^\pm$ exchange; however, in models with two Higgs doublets there is also a contribution from virtual charged Higgs bosons. This process has been studied extensively for the Type-II 2HDM up to next to leading order (NLO) [61] and more recently at next-to-next-to-leading order (NNLO) [62,48,59] for the SM part. The lower bound on the charged Higgs mass is extremely sensitive to the experimental central value and error of the branching ratio. Following the work of Misiak et al. [62] a lower bound on the charged Higgs mass was found to be $M_{H^\pm} \geq$ 295 GeV at the 95% C.L. The constraint on $M_{H^\pm}$ in the lepton-specific model is the same as in the Type-I model since they share the same Yukawa structure in the quark sector and this decay is proportional to $\cot^2\beta$. Varying $BR(b \to s\gamma)$ as a function of $\tan\beta$ a lower bound of $\tan\beta \gtrsim 4$ (2) was found for $M_{H^\pm} = 100$ GeV (500 GeV) in Ref. [25].

In both models, the usual low energy constraining processes used in the Type-II model, $B^+ \to \tau^+\nu$, $D^+ \to \tau^+\nu$, $b \to c\tau\nu$, and $B^0_{(s)} \to ll$, do not give constraints since

the $\cot\beta$ dependence of the charged Higgs coupling to one fermion type cancels with the $\tan\beta$ dependence of the charged Higgs coupling to another fermion type.

4.3 LEP-II Direct Search

Combined limits from the four LEP collaborations have been given for $e^+e^- \to H^+H^-$ with $H^+ \to \tau\nu$ or $c\bar{s}$ and $BR(H^+ \to \tau\nu) + BR(H^+ \to c\bar{s}) = 1$. Lower bounds were placed on $M_{H^\pm}$ as a function of the allowed decay modes of $H^\pm$. In the 2HDM-L, taking $\tan\beta \geq 5$ allows the approximation $BR(H^+ \to \tau^+\nu_\tau) \simeq 1$ for all considered values of $\tan\beta$. This allowed us to use the direct constraint from the OPAL collaboration $M_{H^\pm} \geq 92.0$ GeV [30] with the assumption $BR(H^+ \to \tau^+\nu_\tau) = 1$. In the Flipped model, for values of $M_{H^\pm} \leq 180$ GeV, the dominant decay was shown to be $H^+ \to b\bar{c}$. This meant the $BR(H^+ \to \tau^+\nu_\tau)$-independent direct constraint from ALEPH had to be used which gives the weaker lower bound $M_{H^\pm} \geq 78.0$ GeV [63].

4.4 LHC Search Prospects

In the low mass range $M_{H^\pm} < m_t - m_b$ the main production mode that has been studied in the literature is $q\bar{q} \to t\bar{t} \to \bar{t}bH^+$ where one top quark decays via $t \to bH^+$. For this mass range in the Type-II model, which these studies have been based upon, the charged Higgs is expected to decay via $H^+ \to \tau\nu$ for all values of $\tan\beta \gtrsim 1$. In the lepton specific model, for charged Higgs masses below 180 GeV, the dominant decay for all values of $\tan\beta$ is also $H^+ \to \tau^+\nu$ so the experimental simulations can be applied directly. In order for this search to be useful for the Flipped 2HDM, decays of the charged Higgs to $q\bar{q}$ or specifically $b\bar{c}$ would need to be included in the

experimental search.

For the high mass range the most widely studied search channel for charged Higgs bosons is the inclusive process $gb \to tH^+$ with $H^+ \to tb$. Since the charged Higgs couplings to quarks is the same in the Flipped model and Type-II model, bottom-gluon fusion is the most promising process for discovering H^+ in the Flipped model and the current studies by ATLAS and CMS can be applied directly. It was noted in Sec. 3.4 that the NLO cross section for a charged Higgs of mass $M_{H^\pm} = 200$ GeV and $\tan\beta = 30$ is $\sigma_{tot}(gb \to tH^-) \sim$ 400 fb [66]. This is by far the largest cross section in this model, followed closely only by $W^\pm H^\mp$ associated production with $\sigma(b\bar{b} \to W^\pm H^\mp) =$ 255 fb , $H^\pm A^0$ associated production with $\sigma(pp \to H^+ A^0) \simeq 50$ fb and Drell-Yan pair produced charged Higgs with $\sigma(q\bar{q} \to H^+ H^-) = 26$ fb all for the same parameter values.

In contrast to the Flipped model, electroweak processes dominate in the lepton-specific model. In this model, the suppression of charged Higgs couplings to quarks poses a challenge for discovery at the LHC. The usual processes involving third generation quarks ($W^\pm H^\mp$ associated production and $gb \to tH^-$) will be suppressed by factors of $\cot^2\beta$ so electroweak pair production of charged Higgs and $H^+ A^0$ associated production will be the main search channels, with H^+decaying predominantly to $\tau\nu$. There are currently no experimental studies on any of these processes.

References

[1] C. Amsler et al. [Particle Data Group], Phys. Lett. B **667**, 1 (2008).

[2] S. Glashow, Nucl. Phys. 22 (1961) 579; S. Weinberg, Phys. Rev. Lett. 19 (1976) 1264; A. Salam, in *Elementary Particle Theory*, ed. N. Svartholm (Almqvist and Wiksells, Stockholm, 1969), p. 367.

[3] J. Goldstone, Nuovo Cimento **19**, 154 (1961)

[4] P. W. Higgs, Phys. Rev. Lett. **13**, 508 (1964)

[5] C. Burgess and G. Moore, *The Standard Model – A Primer* (Cambridge University Press, Cambridge, UK, 2007)

[6] J. Goldstone, A. Salam, S. Weinberg, Phys. Rev. **127**, 965 - 970 (1962).

[7] S. Dawson, arXiv: hep-ph/9901280 (1999).

[8] H. E. Haber, G. L. Kane and T. Sterling, Nucl. Phys. B **161**, 493 (1979).

[9] T. D. Lee, Phys. Rev. D **8**, 1226 (1973).

[10] S. Davidson and H. E. Haber, Phys. Rev D **72**, 035004 (2005).

[11] P. Fayet, Nucl. Phys. B **78**, 14 (1974).

[12] S. L. Glashow and S. Weinberg, Phys. Rev. D**15**, 1958 (1977).

[13] E. A. Paschos, Phys. Rev. D**15**, 1966 (1977).

[14] H. Georgi, Hadronic J. **1**, 1227 (1978).

[15] J. F. Gunion, H. E. Haber, G. L. Kane, and S. Dawson, *The Higgs Hunter's Guide* (Westview Press, Boulder, Colorado, USA, 2000), SCIPP-89/13.

[16] P. Fayet and S. Ferrara, Phys. Rept. **32**, 249 (1977).

[17] R. D. Peccei and H. R. Quinn, Phys. Rev. Lett. **38**, 1440 (1977).

[18] R. M. Barnett, G. Senjanovic, L. Wolfenstein and D. Wyler, Phys. Lett. B **136**, 191 (1984).

[19] R. M. Barnett, G. Senjanovic and D. Wyler, Phys. Rev. D **30**, 1529 (1984).

[20] Y. Grossman, Nucl. Phys. B **426**, 355 (1994) [arXiv:hep-ph/9401311].

[21] A. G. Akeroyd and W. J. Stirling, Nucl. Phys. B **447**, 3 (1995); A. G. Akeroyd, Phys. Lett. B **377**, 95 (1996) [arXiv:hep-ph/9603445]; A. G. Akeroyd, Nucl. Phys. B **544**, 557 (1999) [arXiv:hep-ph/9806337].

[22] M. Aoki, S. Kanemura and O. Seto, arXiv:0807.0361 [hep-ph].

[23] H.S. Goh, L. J. Hall and P. Kumar, [arXiv:hep-ph/0902.0814] (2009).

[24] M. Aoki, S. Kanemura, K. Tsumura and K. Yagyu, [arXiv:hep-ph/0902.4665] (2009).

[25] S. Su and B. Thomas, [arXiv:hep-ph/0903.0667] (2009).

[26] A. G. Akeroyd, J. Phys. G **24**, 1983 [arXiv:hep-ph/9803324] (1998).

[27] B. Thomas, "Phenomenology of a Lepton-Specific Higgs", talk presented at the Pheno 2008 Symposium, Madison, Wisconsin (2008).

[28] V. Barger, H. E. Logan, G. Shauhgnessy, Phys. Rev. D **79**, 115018 (2009) [arXiv:0902.0170 [hep-ph]].

[29] H. Logan and D. MacLennan, Phys. Rev. D **79**, 115022 (2009) [arXiv:0903.2246 [hep-ph]].

[30] OPAL Collaboration, [arXiv:hep-ex/08120267] (submitted to Eur. Phys. J), G. Abbiendi *et al.* [OPAL Collaboration], Eur. Phys. J. C **32**, 453 (2004) [arXiv:hep-ex/0309014].

[31] LEP Higgs Working Group for Higgs boson searches, ALEPH, DELPHI, L3, and OPAL Collaborations, arXiv:hep-ex/0107031 (2001).

[32] F. Halzen and A.D. Martin, *Quarks and Leptons* (John Wiley and Sons, USA, 1984); P. Krawczyk and S. Pokorski, Phys. Rev. Lett. **60**, 182 (1988).

[33] W. Hollik and T. Sack, Phys. Lett. B **284**, 427 (1992).

[34] J.M. Roney, Nucl. Phys. B (Proc. Suppl.) **169**, 379-386 (2007).

[35] M. Bona *et al.*, SuperB CDR, arXiv:0709.0451 [hep-ex].

[36] L. Michel, Proc. Phys. Soc. A **63**, 514 (1950); C. Bouchiat and L. Michel, Phys. Rev. **106**, 170 (1957); T. Kinoshita and A. Sirlin, Phys. Rev. **108**, 844 (1957); T. Kinoshita and A. Sirlin, Phys. Rev. **113**, 1652 (1959).

[37] J. Musser, Ph.D. thesis, UMI-32-02340 (2005); W. Fetscher and H. J. Gerber, S. Eidelman *et al.* [Particle Data Group], Phys. Lett. B **592**, 1 (2004).

[38] W. Fetscher, H.J. Gerber, and K.F. Johnson, Phys. Lett. B **173**, 102 (1986).

[39] K. Mursula, M. Roos, and F. Scheck, Nucl. Phys. B **219**, 321 (1983), F. Scheck, Phys. Rept. **44**, 187 (1978).

[40] A. Alves and T. Plehn, Phys. Rev. D **71**, 115014 (2005) [arXiv:hep-ph/0503135].

[41] W. Fetscher and H.J. Gerber, *Precision Measurements in Muon and Tau Decays*, in *Precision Tests of the Standard Electroweak Model* (World Scientific, Singapore, 1995), p. 657-705.

[42] E. Fermi, *NuclearPhysics*. (University of Chicago Press, 1950).

[43] W. S. Hou, Phys. Rev. D **48**, 2342 (1993).

[44] A. Gray *et al.* [HPQCD Collaboration], Phys. Rev. Lett. **95**, 212001 (2005) [arXiv:hep-lat/0507015].

[45] E. Barberio *et al.* [Heavy Flavor Averaging Group], "Averages of $b-$hadron and $c-$hadron Properties at the End of 2007," arXiv:0808.1297 [hep-ex].

[46] B. A. Dobrescu and A. S. Kronfeld, Phys. Rev. Lett. **100**, 241802 (2008) [arXiv:0803.0512 [hep-ph]].

[47] E. Follana, C. T. H. Davies, G. P. Lepage and J. Shigemitsu [HPQCD Collaboration and UKQCD Collaboration], Phys. Rev. Lett. **100**, 062002 (2008) [arXiv:0706.1726 [hep-lat]].

[48] A. Kaffas, P. Osland, O.Ogreid, Phys. Rev. D **76**, 095001 (2007).

[49] H. Logan and U. Nierste, Nucl. Phys. B **586**, 39 (2000) [arXiv:hep-ph/0004139].

[50] J. Hewett, Phys. Rev. Lett. **70**, 1045 (1993) [arXiv:hep-ph/9211256].

[51] G. Yu, *et al.* [CDF Collaboration], CDF note 9322 (2008), available from http://www-cdf.fnal.gov.

[52] DØ Collaboration, DØ Note 5715-CONF (2008), available from http://www-d0.fnal.gov.

[53] A. Abulencia *et al.* Phys. Rev. Lett. **96**, 042003 (2006).

[54] A. Djouadi, J. Kalinowski, M. Spira, Comput. Phys. Commun. **108**, 56 (1998) [arXiv:hep-ph/9704448].

[55] K. A. Assamagan and Y. Coadou, Acta Phys. Polon. B **33**, 707 (2002); Y. Coadou, FERMILAB-THESIS-2003-31.

[56] R. Kinnunen and A. Nikitenko, report CMS note 2003/006 - available from http://cdsweb.cern.ch.

[57] G. Aad *et al.* [The ATLAS Collaboration], arXiv:0901.0512 [hep-ex].

[58] B. Grinstein *et. al*, Nuclear Physics B **339**, 269-309 (1990).

[59] T. Becher and M. Neubert, Phys. Rev. Lett. **98**, 022003 (2007); Phys. Lett, B **633**, 739 (2006); **637**, 251 (2006).

[60] E. Barberio *et. al.* (HFAG), hep-ex/0603003.

[61] M. Ciuchini *et. al*, Nucl. Phys. B **527**, 21 (1998).

[62] M. Misiak *et. al*, Phys. Rev. Lett. **98**, 022002 (2007) [arXiv:hep-ph/0609232].

[63] P. Colas [ALEPH Collaboration], ALEPH Note 2001-016 (2001), available from http://cdsweb.cern.ch/.

[64] M. Acciarri *et al.* [L3 Collaboration], Phys. Lett. B **496**, 34 (2000) [arXiv:hep-ex/0009010].

[65] J. Abdallah *et al.* [DELPHI Collaboration], Eur. Phys. J. C **34**, 399 (2004) [arXiv:hep-ex/0404012].

[66] T. Plehn, Phys. Rev. D **67**, 014018 (2003) [arXiv:hep-ph/0206121].

[67] A. A. Barrientos Bendezu and B. A. Kniehl, Phys. Rev. D **59**, 015009 (1999) [arXiv:hep-ph/9807480].